Improved Well Design with Risk and Uncertainty Analysis

by

John Emeka Udegbunam

Thesis submitted in fulfillment of
the requirements for degree of
PHILOSOPHIAE DOCTOR
(PhD)

Faculty of Science and Technology
Department of Petroleum Engineering
2014

University of Stavanger
N-4036 Stavanger
NORWAY
www.uis.no

ISBN: 978-82-7644-590-9

ISSN: 1890-1387

PhD thesis no. 242

To my lovely wife and children

Contents

Preface iv
Acknowledgements v
Summary vi
List of Papers vii
Abbreviations ix
Nomenclature x

1 Introduction 11
1.1 Well Construction 11
1.2 Conventional Drilling 12
1.3 Innovative Drilling Concepts 13
1.3.1 Managed-Pressure Drilling 14
1.3.2 Underbalanced Drilling 18
2 The Role of Models in Well Planning 21
2.1 Introduction 21
2.2 Wellbore Stability Models 21
2.2.1 In-Situ Stresses 23
2.2.2 Mechanisms of Wellbore Failures 24
2.3 Well Flow Models 25
2.3.1 Model Formulation 26
2.3.2 Numerical Solution 30
3 Stochastic Modeling 33
3.1 Introduction 33
3.2 Risk and Uncertainty 34
3.3 Monte Carlo Simulation 35

3.4 Stochastic Model 37
4 Results and Discussion 39
4.1 Wellbore Stability Analyses 39
4.1.1 Example Cases 41
4.1.2 Stochastic Sensitivity Analysis 45
4.2 Underbalanced Operations 48
4.2.1 Uncertainty BHP Prediction 48
4.2.2 Mechanics of Collapse for UBD 55
4.2.3 Sensitivity Analysis for UBO 58
5 A Transient Model for Well Flows 60
5.1 Introduction 60
5.2 The AUSMV Scheme 61
5.3 Dual-Gradient Drilling 62
5.4 Underbalanced Drilling 67
5.5 Inference 70
6 Overview of the Research Papers 72
7 Conclusion and Further Work 76
7.1 Conclusion 76
7.2 Further Work 77
References 79

Preface

This thesis is submitted in fulfilment of the requirements for the Philosophiae Doctor (PhD) degree. The research was conducted at the Department of Petroleum Engineering, University of Stavanger (UiS), Norway.
All compulsory PhD courses were taken at UiS. Two additional courses were taken at the Norwegian University of Science and technology (NTNU) and University of Bergen (UiB).
The work was carried out from 1 September 2011 to 29 August 2014. The main supervisor was Prof. Kjell Kåre Fjelde, and the co-supervisor was Prof. Bernt Sigve Aadnøy.
The researcher was an employee in UiS throughout this period.

The Norwegian Ministry of Education and Research funded the project. There was a onetime financial support from Statoil through the Akademia program.

The thesis is divided into two parts. The first part comprises seven chapters.
Chapters 1 and 2 present background information relevant to the research.
Chapter 3 discusses stochastic modeling. The chapter describes a fully probabilistic approach for transforming deterministic models to stochastic models. In this case, wellbore stability models and a steady-state hydraulic model are given as the base models.
Chapter 4 presents simulation results and discussion.
Chapter 5 discusses a transient flow model for MPD and UBD applications.
Chapter 6 gives summaries of the research publications.
The last chapter presents the conclusion of the work. The chapter also includes a list of concerns that should be resolved in future studies.

The second part of the thesis consists of five technical papers describing the research findings. A seminar paper that has been prepared for submission to a conference is also included.

Acknowledgements

The Norwegian Ministry of Education and Research funded this work. I thank the ministry for its beneficence.
I also thank Statoil for providing a onetime financial support through the Akademia program.

I thank Prof. Kjell Kåre Fjelde for his generous contribution towards the success of this work. Prof. Fjelde is not only my academic mentor but also a dependable friend, with whom I often share technical and personal challenges. His three years of close supervision of this work has transformed me into a fine petroleum engineer with a strong drive for problem solving.

I also thank Prof. Bernt Sigve Aadnøy for bringing his wealth of experience to bear on this work. Indeed, many inspiring discussions I had with him have enriched the content of the thesis.

My gratitude goes to the management of the Department of Petroleum Engineering. In particular, I appreciate the magnanimous supports I received from the institute leader, Hans Borge, and HR consultant, Kathrine Molde.
I wish to acknowledge my friends and colleagues at UiS, especially those that sat with me in the same office during the PhD period.
I also acknowledge the employees at International Research Institute of Stavanger, whom I worked with, for their contributions.

I am deeply indebted to my amiable wife, Obianuju, and ever-enthusiastic sons, Chidubem and Chinonuju. I thank them for their encouraging smile and unwavering love. I could not have gone this far without the support and prayers of my wife.

Above all, I thank Almighty Chukwu Okike, the Cause of all things visible and invisible, for His sustenance and guidance. His love and grace are ever upon my household.

Chukwuemeka Udegbunam
September 2014

Summary

Uncertainty and associated risk assessment are frequently applied in many disciplines such as engineering, medicine and economics. Yet this study is limited to a quantitative uncertainty analysis with respect to well design, in view of modeling. Well planning is a complex process involving several physical parameters that are decisive for casing design. Some of the input variables that are subject to randomness are considered uncertain parameters. In addition, tools and mathematical models used for well design do not provide true interpretations of natural phenomena or geological processes. The models, also, are subject to the uncertainties, which may result from the approximate nature of the modeling processes. Therefore, it is important to show how these uncertainties affect the model outputs. This information is critical for decision-making during well planning.

Traditionally, deterministic models are used for predicting critical fracturing and collapse pressures required for mud program and casing design. In underbalanced drilling, the operational envelope is predicted based on single-point estimates of pore and collapse pressures. The deterministic method usually neglects the modeling uncertainties.

This thesis proposes an improved methodology for well design. The approach considers uncertainties in the input data and identifies the most critical parameters. The input uncertainties—expressed as probability distributions—are propagated by means of Monte Carlo simulation.
The intent is to provide a systematic way of weighing the deterministic predictions against the results from the stochastic simulations. With the probabilistic approach, it may be easier for well planners to handle contingent well operations.

The work also presents a one-dimensional, two-phase transient model termed the AUSMV scheme. The flow model has some potential that can be relevant to training and academic purposes.
The capability of the scheme to simulate highly dynamic phenomena is presented for dual-gradient drilling and underbalanced operations.

List of Papers

Paper I John Emeka Udegbunam, Kjell Kåre Fjelde, Øystein Arild, Eric Ford, and Hans Petter Lohne. Uncertainty-Based Approach for Predicting the Operating Window in UBO Well Design. Paper SPE 164916**,** presented at the EAGE Annual Conference & Exhibition incorporating SPE Europec, London, UK, 10–13 June 2013.

Paper I was also published in the journal, *SPE Drilling & Completion*.

Paper II John Emeka Udegbunam, Hans Petter Lohne Kjell Kåre Fjelde, Øystein Arild, and Eric Ford. Improved Underbalanced Operations with Uncertainty Analysis. Paper SPE 167954, presented at the 2014 IADC/SPE Drilling Conference and Exhibition, Fort Worth, Texas, USA, 4–6 March 2014.

Paper III John Emeka Udegbunam, Bernt Sigve Aadnøy, and Kjell Kåre Fjelde. Uncertainty Evaluation of Wellbore Stability Model Predictions. Paper SPE 166788, presented at the SPE/IADC Middle East Drilling Technology Conference and Exhibition, Dubai, 7–9 October 2013.

Paper III was also published in *Journal of Petroleum Science & Engineering*.

Paper IV John Emeka Udegbunam, Kjell Kåre Fjelde, Steinar Evje. The Academic AUSMV Scheme — A Simple but Robust Model for Predicting Highly Dynamic Well Flow Phenomena. An extended abstract, presented at the Celle Drilling 2012, Celle, Germany, 17–18 September.

Paper V John Emeka Udegbunam, Kjell Kåre Fjelde, Steinar Evje, Gerhard Nygaard. A Simple Transient Flow Model for MPD and UBD Applications. Paper SPE 168960, in the proceedings of the SPE/IADC Managed Pressure Drilling and Underbalanced Operations Conference and Exhibition, Madrid, Spain, 8–9 April 2014.

Paper V was revised and submitted to *SPE Drilling & Completion*, with a title:
On the AUSMV Scheme: A Simple Transient Flow Model for MPD and UBD Applications.
The paper (**DC-0114-0015.R2**) is presently being given full consideration for publication.

Paper VI John Emeka Udegbunam. Mud Losses in Fractured Carbonate Formations. Presented at the 4th Annual Petroleum Research School of Norway (NFiP) PhD Seminar, Stavanger, Norway, 21 October 2013.
To be submitted to a technical conference.

Abbreviations

AUSM	Advection Upstream Splitting Method
AUSMV	AUSM variant
CBHP	Constant bottomhole pressure
BHP	Bottomhole pressure
BHA	Bottomhole assembly
DGD	Dual-gradient drilling
ECD	Equivalent circulating density
GVF	Gas volume fraction
HPHT	High pressure, high temperature
MPD	Managed pressure drilling
NCS	Norwegian Continental Shelf
NPT	Nonproductive time
PI	Productivity index
PMCD	Pressurized mud-cap drilling
P10	Tenth percentile
P50	Fiftieth percentile
P90	Ninetieth percentile
RCD	Rotating control device
ROP	Rate of penetration
SG, sg	Specific gravity
TVD	Total vertical depth
UBD	Underbalanced drilling
UBO	Underbalanced operations
WSA	Wellbore stability analyses

Nomenclature

A	Annular cross-sectional area [m^2]
a_g	Sound velocity in gas [m/s]
a_l	Sound velocity in liquid [m/s]
d_i	Inner diameter of annulus [m]
d_o	Outer diameter of annulus [m]
C_0	Profile parameter
f	Friction factor
g	Acceleration due to gravity [m/s^2]
N_{Re}	Reynolds Number
P_{cho}	Choke pressure [Pa]
P_o	Pore pressure [Pa]
P_{wc}	Wellbore collapse pressure [SG]
P_{wf}	Wellbore fracture pressure [SG]
V_d	Drift velocity of gas relative to liquid [m/s]
v_g	Velocity of gas [m/s]
v_l	Velocity of liquid [m/s]
α	Angle of internal rock friction [deg]
α_g	Gas volume fraction
α_l	Liquid volume fraction
μ_g	Gas viscosity [Pa.s]
μ_l	Liquid viscosity [Pa.s]
ρ_g	Gas density [kg/m^3]
ρ_l	Liquid density [kg/m^3]
σ_h	Minimum horizontal stress [SG]
σ_H	Maximum horizontal stress [SG]
σ_v	Overburden stress [SG]
τ_o	Cohesive rock strength [SG]

1 Introduction

1.1 Well Construction

Well construction involves drilling through subsurface strata to reach a target zone. The first step in well construction is well planning. This includes casing design, drilling fluid program, bit selection and other related activities. Pore pressure usually increases with depth. Therefore, it is necessary to run casings at interval and weigh up the mud, to avoid kicks and protect the formation further up. The casing is also used for isolating weak or poorly consolidated formations such as sand beds and shale zones. Sometimes, it is very challenging to set casing at a desired depth due to depth uncertainty. There are also uncertainties associated with pore, collapse and fracture pressure prognoses. Failure to manage these uncertainties can lead to wellbore failures such as collapse and fracturing. Eventually, this may lead to stuck pipe or lost circulation. Uncertainty in pore pressure prediction can cause well-control incidents, that is, well kicks. In the worst case, this may lead to blowout.

Studies show that well cost is on the increase, despite cutting-edge technologies developed by the industry in the recent time. This may be partly attributed to a stable, high oil price. Dwindling hydrocarbon reserves—which have forced the operators to venture into harsher and more challenging environments—and an increasing complexity in the well design processes may also be responsible for high well costs.

Fig. 1 presents average well costs on drilling rigs for 8 fields on the Norwegian Continental Shelf (NCS). The report states that well costs on fixed installations have quadrupled in ten year. Within the same period, the costs on mobile drilling units have tripled. Judging by the statistics, one may conclude that the older wells were more cost-effective than the newly drilled wellbores. At this point, three pertinent questions come to mind. What can we learn from the older wells? To what extent can we trust the predictions of the models used in well design? Which processes need to be improved?

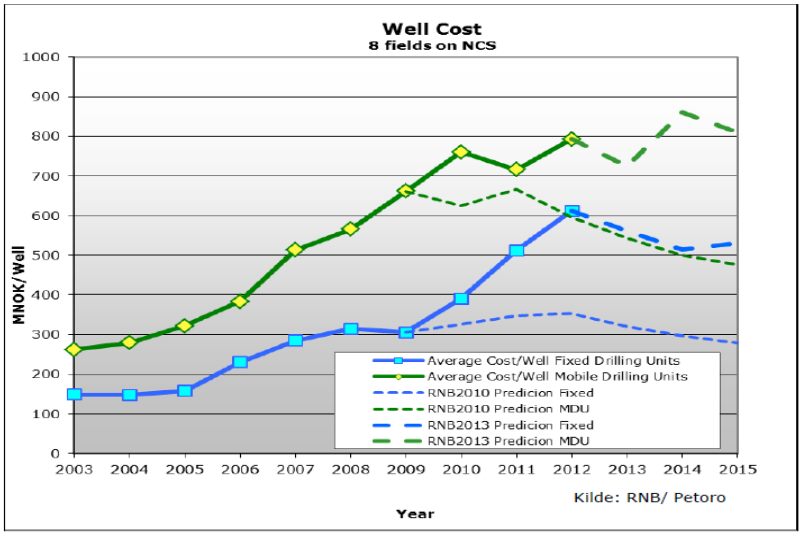

Figure 1.1—Well costs for 8 fields on the NCS between 2003 and 2012 (from Petoro 2014).

The need to improve well design, considering high well costs and modeling uncertainties, has motivated the stochastic method presented in Chapter 3.

1.2 Conventional Drilling

The traditional drilling method has evolved with the oil and gas industry. The method is best suited for non-fractured formations with a wide margin between fracture and pore pressures. In this technique (overbalanced drilling), mud weight is selected such that the well pressure is greater than the pore pressure. This is to prevent entry of the formation fluid into the well. Many factors affect the success of overbalanced drilling operation. The most critical is the mud weight selection. According to Aadnøy (2010), the difference between success and failure is nearly always tied to the mud program. Too low a mud weight may result in collapse and fill problems, while too high a mud weight may result in mud losses or differential sticking. The author also states that stuck pipe and circulation losses are the two most costly drilling problems and may take 10–

20% of the total well time. To minimize the problems, Aadnøy (2010) proposed the median line principle. This states that the mud weight should be kept close to the in-situ stress field in a surrounding rock. The design approach minimizes the risks of lost circulation and differential sticking, because a minimum disturbance is introduced in the borehole wall.

Fig. 1.2 shows typical mud weight selections. The median-line mud weight will provide a common optimum for many key parameters that influence the drilling process. In addition, the mud weight is always a compromise—one optimum at the top and another optimum at the bottom.

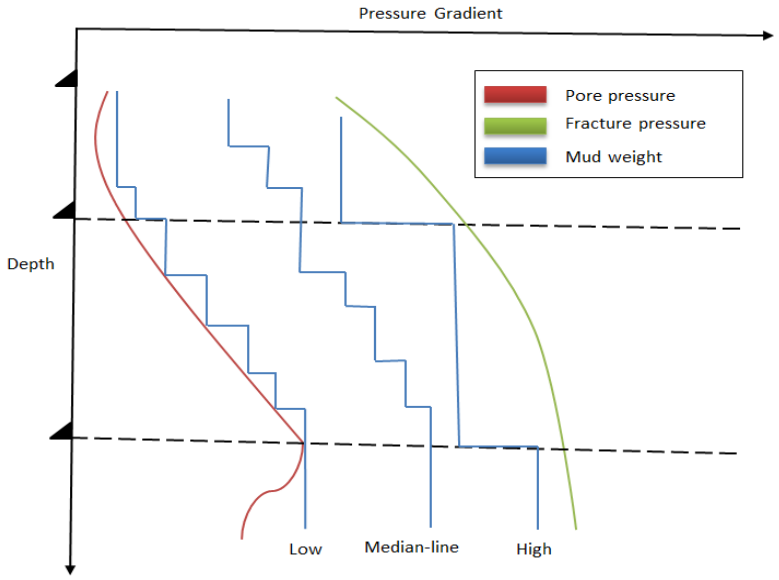

Figure 1.2—Typical mud weight selections (modified after Aadnøy 2010).

1.3 Innovative Drilling Concepts

The two major drilling challenges associated with the conventional drilling technique are circulation loss and stuck pipe. During drilling operation, different types of casing strings (Aadnøy 2010; Rahman and Chilingarian 1995) are set and cemented to the formation at interval. In addition, weak or

troublesome zones are isolated with casings, to prevent interaction between the well and the formation. As the well gets deeper, the diameter of a successive casing becomes smaller until a pay zone is drilled. However, there exist some prospects, where it will impossible to reach the target depths, or where desired production-casing diameter cannot be achieved, by use of the conventional technology (Breyholtz 2011). Such prospects include deep and ultra-deep-water wells. Other problem areas include depleted fields and naturally fractured formations.
Depending on the problem areas, the need to drill deeper with few casings and handle depleted reservoirs, to minimize lost circulation and well kicks, has motived the developments of managed-pressure drilling (MPD) and underbalanced drilling (UBD).

1.3.1 Managed-Pressure Drilling

Some hydrocarbon formations have narrow pressure windows between the pore and fracture pressures. The narrow margins may exist in

- depleted reservoirs, for example, NCS
- deep and ultra-deep-water wells, for example, Gulf of Mexico
- high-pressure, high-temperature (HPHT) fields.

Lost circulation and well kicks are frequently encountered while drilling in these formations. It is also a major drilling problem associated with naturally fractured formations.

MPD technologies make it possible to exploit the prospects that, conventionally, would have been undrillable or difficult to drill. The methods enable drillers to precisely manage the annular pressure profile and ‘walk’ the thin line between the pore and fracture pressures. MPD drastically helps to cut nonproductive time (NPT) by reducing circulation loss, gas kicks, and stuck pipe incidents. MPD also mitigates equivalent circulating density (ECD) problems while drilling extended reach wells and wells with narrow pressure margins. Casing points can be extended, to limit the total number of casing strings and the subsequent hole size reduction (Rehm et al. 2008).

According to the IADC committee on UBO and MPD (Malloy et al. 2009), managed-pressure drilling is an adaptive drilling process used to precisely control the annular pressure profile throughout the wellbore. The objectives are

to ascertain the downhole pressure environment limits and to manage the annular pressure profile accordingly. The intention of MPD is to avoid influx of formation fluids to the surface. Any influx incidental to the operation will be safely contained using an appropriate process.
The MPD process employs a collection of tools and techniques, which may mitigate the risks and costs associated with drilling wells that have narrow downhole environment limits, by proactively managing the annular hydraulic pressure profile. MPD may include control of backpressure, fluid density, fluid rheology, annular fluid level, circulation friction and hole geometry or combination thereof. MPD may allow faster corrective action to deal with observed pressure variations. The ability to dynamically control annular pressures facilitates drilling of what might otherwise be economically unattainable prospects.

1.3.1.1 MPD Techniques

Many MPD systems use a rotating control device (RCD) to enclose the mud return system. Returns flow control is a safety measure to divert gases away from the rig floor. By diverting gases, the RCD avoids having to close the blowout preventer and allows pipe movement while circulating out gas influx (Nas, 2010). The MPD system may include other components such as backpressure pump, choke manifold, non-return valve and separation unit.
The three major MPD techniques are:

Pressurized Mud-Cap Drilling (PMCD). This method refers to drilling without returns to the surface, but with a full annular fluid column maintained above the formation taking the injected fluid and drill cuttings. The PMCD is only applicable in highly fractured and vuggy carbonates where there is a high tendency for the mud to be lost to the formations. In this method, a sacrificial fluid is pumped down the drill pipe during drilling, and the returns are pumped back into the loss zone along with the cuttings (Rehm et al. 2008). In addition, a light annular fluid is used in the upper part of the annulus above RCD. The pressure at the RCD is closely monitored. If the pressure increases, it is an indication of a migrating kick. In this case, the kick will be pumped back into the formation, to maintain well control.

Constant Bottomhole Pressure (CBHP). This is a wellbore-pressure management technique aimed at maintaining constant well pressure at critical positions in a well. This includes measures taken to control ECD or annular friction, to keep the bottomhole pressure (BHP) within the operational window between the downhole pressure limits. The method is similar to the Driller's Method used in conventional drilling to circulate out kicks while keeping the BHP constant.
During pipe connections, annular pressure will decrease due to loss of the friction pressure component. Circulation across choke by means of backpressure pump is used to maintain the desired BHP, and to avoid kicks. An automated CBHP (Osayande et al. 2014) was recently applied in drilling a steam-assisted-gravity-drainage well with a tight drilling window.

Dual-Gradient Drilling (DGD). The DGD technique is mainly used for deepwater applications. This involves the use of two different drilling fluid gradients in a well. In some cases, the marine riser may be displaced with seawater, hence eliminating the mud column between the rotary table and the seabed (Nas 2010). One major advantage of having a seawater-filled riser and dual-gradients, as compared with conventional riser drilling, is that the riser margin is always maintained, even in emergencies (Schubert et al. 2006). In DGD, the annular pressure profile follows a curved pattern, because the drilling fluid density varies along the annulus (Breyholtz 2011).
The dual gradient effect can be created by dilution of mud with lightweight solid additives (Cohen and Deskins 2006), to reduce the mud density, or by injection of gas into the riser (Lopes and Bourgoyne 1997), to lower the mud density down to seawater values.

Recent DGD concepts incorporate mudlift system. In these systems, the returning mud is not conducted through the marine riser, but is circulated back to the surface through a separate return line.
One of the DGD systems uses a riser that is partly filled with mud. In this concept, the mud level in the riser is adjusted by means of a subsea pump such that the air-mud interface exists below the sea level, but above the sea floor. During drilling operation, the mud level must be adjusted when the circulation rate is changed, to maintain the desired BHP. This system is described in Fossli and Sangesland (2006) and Falk et al. (2011). A field application of the system

is described in Rajabi et al. (2012). In addition, Handal, (2011) discusses general well-control procedures for this type of DGD system.
The second type of DGD system operates with a riser that is displaced with seawater. An example of such system is the SubSea MudLift Drilling (SMD) system. The concept is described in Eggemeyer et al (2001), Schumacher et al. (2001) and Schumacher et al. (2002). A full-scale field deployment of the SMD system is presented in Dowell (2010). The well control procedures for this system are given in Shubert et al. (2006).
In addition, another category of DGD system is designed to operate riserless. This concept is discussed in Stave et al. (2005) and Brown et al. (2007).

The earliest SMD concept was designed to be riserless, but it is now being deployed with a conventional riser. Then it is required that the seawater in the riser annulus is isolated from the mud in the lower part of the well. A subsea rotating diverter, which is run through the riser and landed at the mud line on the seabed, provides the line of separation. The device is similar to RCD, though it not considered a component of the well control system. Here, a subsea pump causes the dual-gradient effect because it is designed to reduce annular pressure just below the subsea rotating control head.
The SMD system is associated with U-tube effect (Eggemeyer et al 2001). However, a drill-string value is placed in the bottomhole assembly (BHA) near the bit to manage this effect.
Fig. 1.3 gives plots of TVD versus pressure for an SMD system.

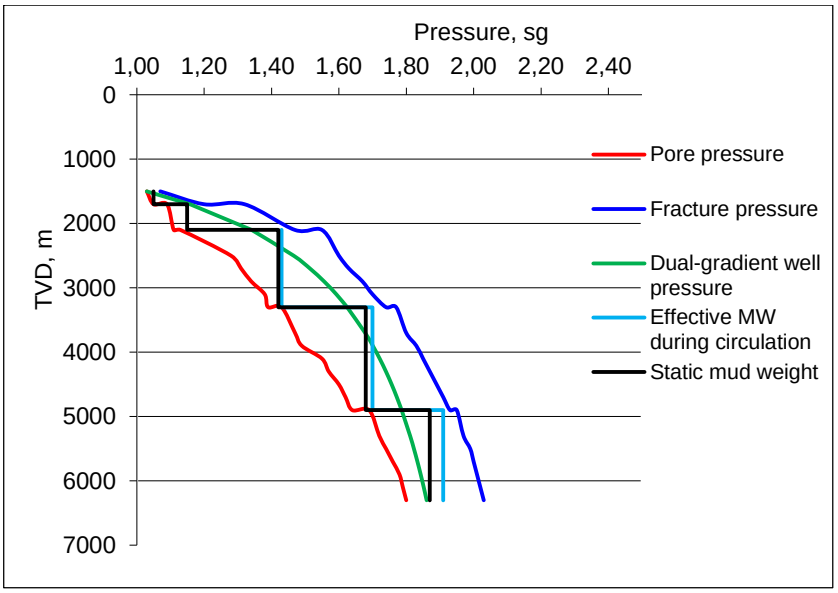

Figure 1.3—Total vertical depth versus pressure, for a typical SMD system. Seawater depth = 1500 m, gradient = 1.03 sg. Mud gradient = 2.12 sg. MW = mud weight.

The MPD system is more expensive compared with the conventional drilling. Yet it delivers significant cost savings by cutting NPT associated with kicks, losses, and well-control events, increasing rate of penetration (ROP) and making previously undrillable wells drillable. Operators find that using MPD cuts their NPT from 20 to 100%. The system usually requires only minor modifications to the conventional rig. It permits all drilling, logging and completion operations to be executed safely and efficiently (Nas, 2010).

1.3.2 Underbalanced Drilling

Underbalanced drilling is not a new technology. The technique was applied in the past because all wells drilled with cable rigs—before the introduction of rotary drilling—were drilled underbalanced (Ramalho and Davidson 2006). The UBD system is a closed-loop drilling system similar to CBHP, with additional separation capacity. However, while MPD systems avoid well kicks, the UBD technique deliberately allows influx of the formation fluid into the wellbore. Underbalanced drilling, essentially, is drilling with BHP less than the

formation or pore pressure. The system allows hydrocarbon production while drilling. It also involves the use of aerated drilling fluids. Typically, the operation can be performed with a drilling fluid (usually hydrocarbons or water) mixed with nitrogen gas or air, or foam. The gas can be injected through the drill string or directly into the annulus—a method called parasitic or concentric annulus injection. In flow drilling, a low-density mud is sufficient to make the well flow.

The UBD technique is applicable in situations where there are potentials for severe fluid loss or total lost circulation (Bennion and Thomas 1994). These include highly fractured formations, vuggy carbonates or karsts, and over-pressured reservoirs. The method can also be used for handling small pressure margins and depleted reservoirs. In horizontal wells (Gough et al. 2011), pore pressure may exceed fracture pressure at some points along the horizontal section. Because of the pressure variations, UBD can be used while drilling the reservoir section, to avoid losses and invasion of the pay zone with foreign materials.

Underbalanced operations (UBO) involve highly dynamic phenomena. There is a need for an efficient multiphase circulating system and a proper modeling of the UBD system, to determine the operating parameters and design procedures. The BHP must be less than the pore pressure but greater than the collapse pressure in the target reservoir section. An overbalanced situation will destroy the intention.

The technique combines drilling and production, hence well control becomes flow control (Saponja 1998). Therefore, the control of BHP is very important for a successful operation. Saponja (1998) shows that a circulating system operating in a friction-dominated region is more stable and beneficial for controlling gas inflow from the reservoir.

The advantages and disadvantages of UBD are outlined in Bennion et. al (1998). The drilling technology aims to avoid lost circulation and eliminate formation damage associated with the conventional overbalanced drilling. Other advantages include improved reservoir productivity, real-time reservoir characterization, and increased rate of penetration. For instance, UBD technique was applied in drilling a deviated well with 60° slant, to improve drilling performance and reduce formation damage (Cunha and Rosa 1998).

To maximize the benefits of UBO, a comprehensive knowledge of the geology and petrophysical characteristics of a candidate reservoir and effective

multiphase system are required. In addition, government regulations and environmental concern must be taken into consideration.

2 The Role of Models in Well Planning

2.1 Introduction

Models are developed to approximate or mimic systems and processes of different natures and of varying complexity. Many processes are so complex that physical experimentation is too time-consuming, too expensive, or even impossible. Therefore, to investigate systems and processes, investigators often turn to mathematical or computational models (Saltelli et al. 2008).

Well planning and subsequent drilling operations require the use of models. These come in form of wellbore stability models and hydraulic models for calculating well pressures. The hydraulic models are further subdivided into steady-state and transient models.

The models, however, have some limitations because the modeling processes only approximate physical phenomena. There also uncertainties related to the model input parameters. Thus, modelers should be aware of the imprecision of these models. In this chapter, the mathematical models used in the present research will be discussed.

Stochastic modeling will be presented in the Chapter 3. The chapter describes how to transform the deterministic models to stochastic models.

2.2 Wellbore Stability Models

Wellbore stability analyses (WSA) became much more imperative at the time the industry began to drill highly inclined wellbores and horizontal or extended reach wells. The results of the analyses are very crucial to casing and cementing operations, especially now the operators have ventured into more challenging environments as deep and ultra-deep waters. This is also important for the exploitation of depleted reservoirs and fractured carbonates.

Borehole instabilities are expected when drilling through shales and unconsolidated sand beds, leading to breaking of rock fragments or collapse situation. The wellbore failures may also be encountered in highly fractured formations and HPHT fields with narrow margins.

One of the main purposes of WSA is to estimate the upper and lower pressure limits (Aadnøy and Chenevert 1987; Mostafavi et al. 2011). These limits are

different for different drilling applications. For overbalanced drilling, fracture and pore pressure profiles represent the upper and lower limits respectively. In UBD, pore pressure profile is the upper limit, while collapse pressure profile is the lower limit.

According to Aadnøy et al (2009), wellbore instabilities include such phenomena as:

- breaking of intact rock around the wellbore due to high stress concentration or sudden temperature variations
- loosening of rock fragments
- fracture extensions from the wellbore into the formation
- failure of rock around the borehole due to interaction with drilling fluid
- squeezing of soft rocks such as salt and shales into the wellbore
- activation of pre-existing faults that intersect the wellbore.

Bradley (1979) summarized the stressed-induced borehole failures as (i) borehole size reduction due to the plastic flow of soft rocks into the wellbore, (ii) borehole enlargement because of brittle rock failure and cavings, and (iii) fracturing resulting from tensile rock failure due to excessive mud pressure.
For a given drilling operation, whether the wellbore failures will occur or not depends on the mud weight selection. Thus, this factor is the most critical determinant influencing the success of any drilling applications. Too low a mud weight may lead to stuck pipe. Too high a mud weight may cause drilling problems such as wellbore fracturing, lost circulation, and differential sticking. Then it is the desire of every driller to use optimal mud weight, to minimize these problems and, subsequently, cut NPT and well costs.

Both casing design and mud program are based on the outcomes of WSA. The wellbore stability models predict critical fracturing and collapse pressures. These are important factors in mud weight selection and casing design. Usually, the predictions of the models are not accurate. Wellbore failures and well control incidents are often due to uncertainties in the geopressure prognoses. The main sources of the uncertainties will be discussed in the subsequent chapter.

2.2.1 In-Situ Stresses

Knowledge of the in-situ stress field is a key factor in the analyses of borehole problems such as fracturing, circulation loss, well collapse and sand production (Aadnøy 1988).

Formations are generally classified as either normally stressed or tectonically stressed, based on the in-situ stresses (Bradley 1979). In relaxed sedimentary basins, the maximum in-situ stress, σ_1, is vertical. This stress is equal to overburden stress, σ_v. The two other principal stresses (σ_2, σ_3) are located in a horizontal plane, and are equal or nearly equal.

Tectonic stresses include stress conditions, which are not considered normally stressed. Tectonically active regions are often associated with areas having active faults, salt domes or foothills. In these regions, the principal in-situ stresses are not necessarily oriented in the vertical and horizontal directions, but may be rotated through significant angles. In addition, the magnitudes of the three principal in-situ stresses are usually different (Bradley 1979).

Usually, the stress concentration around the borehole wall is very high. This effect decreases rapidly away from the wellbore. At a distance away from the wall, the principal in-situ stresses are undisturbed and lie along their in-situ directions. The normal stresses around the wellbore wall are defined as radial, σ_r, tangential, σ_θ, and axial, σ_z, stresses (Aadnøy 2009).

The magnitude of the overburden stress can be estimated from bulk density measurements. At deeper depth, density or sonic logs are often used for the stress estimation (Aadnøy 2011).

Leak-off test (LOT) data can be used to estimate the magnitudes of the horizontal stresses. Alternatively, extended LOT (XLOT) can be used. The XLOTs and LOTs are mainly performed in shale and mudstone, which generally have the highest stress and fracture gradients (Addis et al. 1998). While it is often common to assume that the magnitudes of the two horizontal in-situ stresses are equal, a new method called inversion technique (Aadnøy 1988) distinguishes between the two stresses. The input data are the LOT fracturing data. The model estimates the magnitudes and directions of the two horizontal stresses from the fracturing data. This method uses stress transformation equations (Aadnøy and Hansen 2005) to take advantage of the directional characteristics of offshore boreholes.

2.2.2 Mechanisms of Wellbore Failures

The two well-established mechanisms that cause wellbore instabilities are shear and tensile failures (Bradley 1979; Aadnøy and Chenevert 1987). The rock failure modes will not be discussed in detail, but the basic concepts are encapsulated. In this work, the formation around the wellbore is assumed linearly elastic. Therefore, other rock deformation properties, for example elastoplasticity, have been neglected. In addition, only vertical well configuration is considered.

Tensile Failure. Formations are generally weak in tension. Bradley (1979) assumed zero tensile strength for rocks and used zero effective stress as a criterion for tensile failure. A vertical fracture will initiate at the wall when the hoop stress goes into tension. The criterion follows that the effective principal stress is less than or equal to zero.
Wellbore fracture results from using too high a mud weight. At any depth interval, defining optimal mud weight that will maintain the gauge hole without fracturing the wellbore is the most challenging aspect of WSA. This largely depends on the accuracy of critical fracturing and collapse pressure predictions. For unequal horizontal in-situ stresses (σ_h, σ_H), the non-penetrating Kirsch model for fracturing pressure (Bradley 1979; Aadnøy and Chenevert 1987) is given by Eq. 2.1.

$$P_{wf} = 3\sigma_h - \sigma_H - P_o \tag{2.1}$$

The equation generally underestimates the fracture pressure, depending on the values of the horizontal in-situ stresses. The problem can be best resolved if an assumption of perfect filter cake (zero filter loss) is made when applying the model (Aadnøy 2010).

Shear Failure. The von Mises Yield Condition and Mohr-Coulomb Shear Failure Criterion are the most commonly used hypotheses for shear failure analysis. However, the discussion will be limited to Mohr-Coulomb Criterion, which is the model adopted for wellbore collapse.
Formations at depth exist under a state of compressive in-situ stress (Bradley 1979). Wellbore collapse is often caused by shear failure of rock around the

borehole. To keep the rock from failing during drilling operation, mud pressure must be sufficiently high, to support the load imposed on the borehole wall by the in-situ stresses. The mud pressure must not be too high as to fracture the formation.

The Mohr-Coulomb failure model for borehole collapse neglects the intermediate principal stress but include the effect of the directional strengths of shales (Aadnøy and Chenevert 1987). The model predicts the minimum mud pressure that can cause wellbore collapse.

Eq. 2.2 gives the shear failure model for collapse.

$$P_{wc} = \frac{1}{2}(3\sigma_H - \sigma_h)(1-\sin\alpha) + P_o \sin\alpha - \tau_o \cos\alpha \qquad (2.2)$$

The equation expresses the collapse gradient in terms of the horizontal stresses , pore pressure, rock friction angle, and cohesive rock strength.

2.3 Well Flow Models

Flow modeling is an integral and important aspect of planning and execution of underbalanced operations. Both steady state and transient models or simulators are available. The models are used for calculating downhole pressure and other flow variables. Because UBD involves a multiphase system, such calculations cannot be done analytically.

The steady-state models predict the UBD operational window. The operational window is a plot of annular BHP versus gas-injection rates for a given liquid rate. This may also include gas-injection limits, depending on the cutting transport and downhole motor requirements.

Fig. 2.1 is a typical UBD operational window. During underbalanced operations, the BHP must stay within the operational limits defined by the pore and collapse pressures.

Well planners use the dynamic models (Rommetveit et al. 1999; Lage 2000; Fjelde et al. 2003; Lage et al. 2003; Mykytiw et al. 2004; Rommetveit et al. 2004; Udegbunam et al. 2014) to gain insights into dynamic well behaviors such as unloading, connections, surge and swab and temperature effects.

In this chapter, the discussion will be limited to two-phase, steady-state flow modeling. This model forms the basis of the stochastic modeling of UBO. The transient flow modeling will be discussed in Chapter 5.

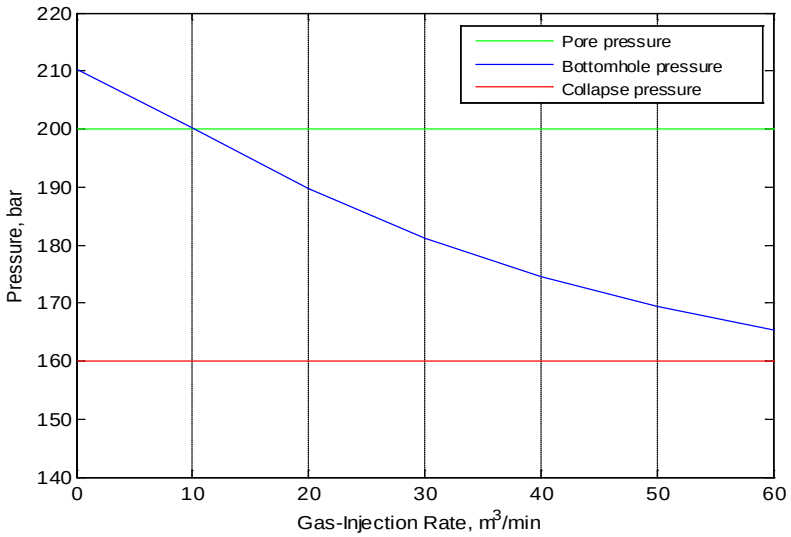

Figure 2.1—A typical underbalanced drilling operational window.

2.3.1 Model Formulation

The governing equations are based on mass and mixture momentum conservations for liquid and gas phases. The two-phase model is simplified with basic assumptions. The flow is considered one-dimensional. It is assumed that there is no mass exchange between the two phases. In addition, the fluid flow along the wellbore is assumed isothermal. Hence, the temperature effects and energy balance equation are eliminated. The isothermal condition, however, does not apply to real or field situation where temperature effects must be included.

$$\frac{\partial}{\partial z}(A\rho_l\alpha_l v_l) = 0 \tag{2.3}$$

$$\frac{\partial}{\partial z}(A\rho_g\alpha_g v_g) = 0 \tag{2.4}$$

$$\frac{\partial P}{\partial z} = -(\rho_l \alpha_l + \rho_g \alpha_g) g - \frac{\Delta P_f}{\Delta z} \tag{2.5}$$

Eqs. 2.3 and 2.4 represent the steady-state mass transport of liquid and gas. This means that mass rate of each phase is constant along the well.
Eq. 2.5 represents the conservation of total momentum of the fluid mixture. It expresses the annular well pressure as a combination of hydrostatic pressure gradient and frictional effects.
This system of equations will be solved for each cell in a discretized well. The solution procedure will be described in detail in Section 2.3.2.

Closure Laws. From the three conservation equations, the unknowns are the liquid and gas volume fractions, designated as α_l and α_g; phase velocities, v_l and v_g; phase densities, ρ_l and ρ_g; and the wellbore pressure, P. This implies that there are three equations but seven unknowns. To find a solution to the system, four additional constraints or closure laws are required.
Eqs. 2.6 through 2.8 represent phase densities and volume fraction relation.

$$\rho_l = \rho_{l,0} + \frac{(P - P_{atm})}{a_l^2} \tag{2.6}$$

$$\rho_g = \frac{P}{a_g^2} \tag{2.7}$$

$$(\alpha_l + \alpha_g) = 1 \tag{2.8}$$

The constants, $\rho_{l,0}$ = 1000 kg/m^3 is the density of liquid at standard conditions, P_{atm} = 1bar (10^5 Pa.) is the atmospheric pressure, a_l = 1000 m/s is the sound velocity in the liquid phase, and a_g = 316 m/s is the sound velocity in the gas phase. The sound velocity is related to the compressibility of the fluid.

The two-phase flow is a highly dynamic phenomenon. This is due to the tendency of gas to move faster than liquid and varying flow patterns, which dependent on the gas volume fraction (GVF).
For a gas-liquid flow in a vertical pipe, Zuber and Findlay (1965) expressed the velocity of gas as the sum of centerline velocity and the drift velocity of gas relative to liquid. The slip equation is of the form,

$$v_g = C_0 v_m + V_d = C_0(v_{ls} + v_{gs}) + V_d \rightarrow C_0(\alpha_l v_l + \alpha_g v_g) + V_d \tag{2.9}$$

where v_g is the gas velocity, C_0 is a profile parameter or distribution coefficient, v_m is average mixture velocity, v_{ls} is superficial liquid velocity, v_{gs} is superficial gas velocity, and V_d is the drift velocity of gas relative to liquid.

Both coefficients, C_0 and V_d, are flow-dependent parameters. Eq. 2.9 is also valid for a vertical liquid-gas flow in an annulus.
The gas phase moves faster than liquid because of two mechanisms:(i) higher concentration of gas near the center of a pipe, where velocity is higher, with the effect captured by the centerline velocity, $C_0 v_m$, and (ii) the tendency of the gas to rise in the pipe due to buoyancy, given by V_d (Livescu et al. 2009). The values of C_0 ranges from 1.0 to 1.2 for most vertical flow patterns such as bubble, dispersed bubble, churn and slug flows. The values of the parameter, V_d, may typically range from zero to 0.55 m/s.

For the dispersed bubble flow, C_0 = 1.0, whereas V_d = zero, that is, no-slip conditions. This occurs at high superficial liquid velocities, whereby turbulent forces break large bubbles and disperse the gas phase in a continuous stream of liquid. This can even occur for GVFs larger than 0.25 but not exceeding 0.52 (Lage and Time 2000).
Higher GVFs cause transition to slug flow. For the slug flow, the conditions for the rise of the Taylor bubble are given by C_0 = 1.2 and $V_d = 0.35\ (g\ (d_o + d_i))^{0.5}$ (Lage and Time 2000).
In the bubble flow, the C_0 values in the range of 1.0 to 1.1 have been mentioned in the literature according to Lage and Time 2000.

Frictional pressure-loss gradient is estimated with Eq. 2.10. Eq. 2.11 gives an expression for calculating the hydrostatic pressure-loss gradient. The equations are based on the drift-flux formulation, where flow condition is assumed homogeneous, and the variables are averaged over a cell or well segment.

$$\frac{\Delta P_f}{\Delta z} = \frac{2 f \rho_m v_m abs(v_m)}{(d_o - d_i)} \tag{2.10}$$

$$\frac{\Delta P_h}{\Delta z} = \rho_m g \tag{2.11}$$

The parameter, f, is friction factor, g is the acceleration due to gravity, z is vertical coordinate along the flow direction, and d_o and d_i are outer and inner diameters of the annulus respectively.

A dimensionless quantity, the Reynolds number, N_{Re}, is the ratio of inertia forces to viscous forces. The quantity is used to distinguish among different flow regimes.
Eq. 2.12 is an expression for the N_{Re}.

$$N_{\mathrm{Re}} = \frac{\rho_m abs(v_m)(d_o - d_i)}{\mu_m} \tag{2.12}$$

Eqs. 2.13 through 2.15 give the multiphase mixture variables: mixture velocity, mixture density, and mixture viscosity.

$$v_m = v_{ls} + v_{gs} = \alpha_l v_l + \alpha_g v_g \tag{2.13}$$

$$\rho_m = \alpha_l \rho_l + \alpha_g \rho_g \tag{2.14}$$

$$\mu_m = \alpha_l \mu_l + \alpha_g \mu_g \tag{2.15}$$

For $N_{\mathrm{Re}} \geq 3000$, the flow is turbulent, and the friction factor is defined by:

$$f = 0.052(N_{\mathrm{Re}})^{-0.19} \tag{2.16}$$

For $N_{\mathrm{Re}} \leq 2000$, the flow is laminar, and the friction factor is given as:

$$f = \frac{24}{N_{\mathrm{Re}}} \tag{2.17}$$

Eq. 2.16 is a Blasius-type equation for calculating friction factor in turbulent flow. The coefficients in the equation may vary, and as pointed out in Caetano (1986), they are experimentally determined.

Eq. 2.17 is used for estimating the Fanning friction factor, for laminar flow in a concentric annulus. The proposed correlation is given in Caetano (1986).

Interpolation is used in calculating friction factor for intermittent flow, where $2000 < N_{\mathrm{Re}} < 3000$, to avoid numerical instability.

2.3.2 Numerical Solution

The numerical solution is based on the Bisection Method described in Gerald and Wheatley (2004). With the shooting technique, the solver estimates primitive variables such as wellbore pressure and phase velocities for each cell, by solving Eqs. 2.3 through 2.9.

The hydraulic model is coupled to a reservoir productivity submodel (Eq. 2.18), to include reservoir inflow.

$$Q = PI(P_o - P_b) \tag{2.18}$$

The parameter, Q, is inflow rate of a reservoir fluid, PI is productivity index, P_o is pore pressure, and P_b is annular bottomhole pressure.

The annular pressure can be expressed as the sum of hydrostatic pressure, pressure loss due to frictional effects, and pressure differential across the choke. A good combination of fluid rates and choke pressure is required, to maintain an underbalanced condition in a target section.
Eq. 2.19 gives the annular BHP in terms of the three components. The pressure component due to the fluid acceleration is not considered because it is negligible.

$$P_b = P_h + P_f + P_{choke} \tag{2.19}$$

Solution Algorithm. The well is discretized into N segments. The flow variables are resolved along the vertical direction denoted by z.
Fig. 2.2 provides a schematic of the discretization procedure.

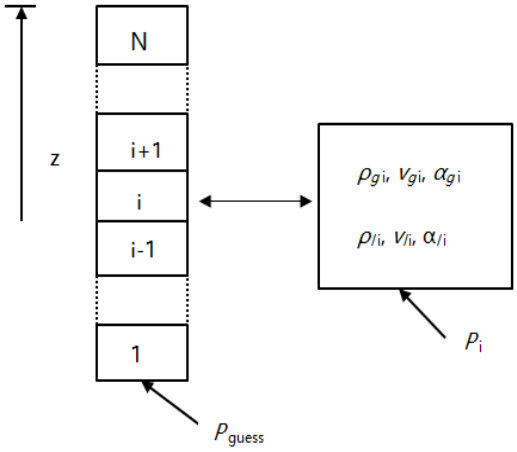

Figure 2.2—A schematic representation of the discretized vertical wellbore (modified after Livescu et al. 2009).

A pressure, P_{guess}, is guessed at the lower boundary of the first cell. The phase densities in this cell are calculated based on the pressure value.
At the injection point (well bottom), the fluid-mass rates, q_l and q_g, are known. With these values, the phase superficial velocities are calculated by use of Eqs. 2.20 and 2.21.

$$v_{ls,1} = \frac{q_l}{A\rho_l(P_{guess})} \tag{2.20}$$

$$v_{gs,1} = \frac{q_g}{A\rho_g(P_{guess})} \tag{2.21}$$

Gas velocity, $v_{g,1}$, is calculated with Eq. 2.9. The phase volume fractions and liquid velocity are determined by solving Eq. 2.22 through 2.24.

$$\alpha_{g,1} = \frac{v_{gs,1}}{v_{g,1}} \tag{2.22}$$

$$\alpha_{l,1} = 1 - \alpha_{g,1} \tag{2.23}$$

$$v_{l,1} = \frac{v_{ls,1}}{\alpha_{l,1}} \tag{2.24}$$

The numerical solver estimates the pressure in the next cell by considering the pressure drops across the previous cell. The frictional and hydrostatic pressure-loss gradients are calculated with Eqs. 2.10 and 2.11.
Then the pressure in cell, *i*, is given by Eq. 2.25

$$P_i = P_{i-1} - \Delta z\left(\frac{\Delta P_{h,i-1}}{\Delta z} + \frac{\Delta P_{f,i-1}}{\Delta z}\right) \tag{2.25}$$

Again, based on the value of P_i, the phase densities, superficial velocities, velocities, and volume fractions in this cell are obtained by solving the mass conservation laws (Eqs. 2.3 and 2.4) and constraints (Eqs. 2.6 through 2.9)
The same algorithm is followed in calculating the pressure and other flow variables in the next cell until the outlet pressure, P_N, in the last segment is estimated. An exact solution must satisfy the function expressed in Eq. 2.26. If not, the solver repeats the iteration once again until a solution is found. The principle is to ensure that the numerical solution satisfies the physical reality.

$$G(P_{guess}) = P_N - P_{cho} = 0 \tag{2.26}$$

However, a tolerance limit, tol = 1000 Pa, is specified in the solver such that if $G(P_{guess}) < \text{tol}$, then the guessed pressure, P_{guess}, is the real bottomhole pressure.

The two-phase flow model is also described in the Papers I and II. The model forms the basis for the uncertainty prediction of UBD operating window presented in Chapter 4.

3 Stochastic Modeling

3.1 Introduction

Physical and geologic models are the bases for constructing mathematical models. While the physical model is a tangible object that represents a natural phenomenon or process, the geologic model is an abstract formulation of a geologic concept that may be tested by collecting geologic data (Koch and Link 1980). Modeling geological processes is subject to uncertainty because of scarcity and inaccurate nature of input data (de Rocquigny et al. 2008). Deterministic models are mainly used in the industry, but they do not consider uncertainty propagation. The problem with these models is that they usually involve single-value assessments of averages or expected values, which effectively obscure risk (Nersesian 2013). An over-simplification of input parameters results in loss of variability information and inability to analyze the associated uncertainties and risks quantitatively (Liang 2002).

Uncertainty-based methods for drilling and well design (Morita 1995; Ottesen et al. 1999; Liang 2002; de Fontoura et al. 2002; Sheng et al. 2006; Aadnøy 2011) are not relatively new concepts. The industry frequently uses scenario analysis to predict the most likely, the best and the worst cases through project cycles. Traditionally, sensitivity analysis is used to ascertain the contributions of input-parameter uncertainties to output uncertainties. The method is often used in hydrocarbon volumetric estimation and well forecasting. One limitation of this approach is that the determining factors, for example, price may fluctuate from time to time. Thus, it will not adequately capture the possible range of the variable distributions.

As quoted in Nersesian (2013), risk lies in the tail of a probability distribution. Only by making the transformation from deterministic and scenario models to stochastic models can one evaluate risk hidden in the tail.
A novel stochastic modeling approach is proposed here. This shows how to propagate uncertainties from assessable input parameters to output realizations. Monte Carlo technique provides a means for the uncertainty propagation. With the approach, the deterministic models presented in Sections 2.2 and 2.3 are transformed to stochastic models. Although the relationships among the variables in the deterministic models are easily predictable, introduction of one or more random elements alters the relationship. Then, instead of having single-

point estimates, the models (now stochastic) predict outputs that follow probability distributions. This idea forms the basis of the stochastic modeling.

3.2 Risk and Uncertainty

The words 'risk' and 'uncertainty' are sometimes used interchangeably and are synonymous with decision-making. An economist, Frank H. Knight, in 1921 distinguished between the two. According to the economist, risk deals with randomness with knowable probabilities, whereas uncertainty deals with randomness with unknowable probabilities. Therefore, while risk is measureable, uncertainty is not (Nersesian 2012). Moors (2011) also defined risk as any threat to the priorities, security or overall integrity of a system. Then risk is a departure from expectations and can have downside or upside consequences (Nersesian 2013). For instance, an operator may expect 100 dollars per barrel of oil. Here, the risk is any price other than 100 dollars, that is, a departure from the expectation. Risk also depends on viewpoints. While the industry views risk in terms of high well costs and low oil price, the society is mainly concerned about high fuel prices and environment pollutions resulting from hydrocarbon activities.

Among the major contributors to the cumulative uncertainties in the model outputs, uncertainties in the input variables rank the highest.

The input-parameter uncertainties may result from measurement errors, absence of information and poor understanding of the driving forces and mechanisms (Saltelli et al. 2008). Where input data are scarce, interpolations and assumptions are often introduced in the model.

Other sources of input uncertainties include chance phenomenon, epistemic uncertainty or lack of knowledge and variability (de Rocquigny 2009).

The output uncertainties may result from the modeling processes because mathematical models only mimic or approximate physical phenomena.

In summary, the modeling uncertainties result from input uncertainties and the uncertainties related to the modeling processes.

Because some input variables are subject to randomness, it will be prudent to treat them as uncertain parameters, with assumed probability distributions. The distributions, according to Saltelli et al. (2008), are valuable because they

represent the modeler's knowledge (or lack of it) regarding the system and its parameterization.

3.3 Monte Carlo Simulation

Monte Carlo method has become a preferred statistical-based tool for well forecasting. The technique has been applied in well time and cost estimation (Williamson et al. 2006; Løberg et al. 2008; Adams et al. 2010), well control (Arild et al. 2008; Arild et al. 2009); UBD well planning (Udegbunam et al. 2013b), and reserve forecast (Murtha 1997).

Monte Carlo simulation yields probability and value relationships for key parameters (Murtha 1997). The technique can propagate uncertainty from assessable variables to output realizations required for decision-making (Bratvold and Begg 2010). A full simulation involves several trials in which random numbers are drawn from independently distributed input variables and are combined together. The results are then presented in form of an output distribution or histogram. This uncertain outcome serves as a guide for defining confidence level and selection of critical parameters, as to optimize risk and uncertainty.

Despite the scope and potentials of this statistical tool, Williamson et al. (2006) advised the users to be wary of its pitfalls. One of such pitfalls is defining the minimum and maximum distribution values from the minimum and maximum of offset data. The extremes of a distribution must be wider than the extremes of a data set it is modeling. Another pitfall is choosing the mean or median of the data set as the distribution most likely value. To avoid the two sources of error, the distribution must have the same mean and standard deviation as the data set.

Input Distributions. Random input variables can be modeled with different types of probability distributions such as uniform, triangular, Gaussian, lognormal and weibull distributions. The properties of the distributions can be found in Walpole et al. (2012).

A real distribution can be constructed if there are many measured or field data. If not, a distribution that best describes the data set can be assumed.

The choice of a distribution shape may differ, depending on applications and data availability. Engineers commonly use the Gaussian or normal distribution. Yet the tails of the distribution may go outside the range of the real data set it is representing. Williamson et al. (2006), however, argued that engineers should not waste time debating on the choice of distribution types. Instead, one should ensure that the correct mean and standard deviation are used. The distribution should also have a range consistent with the data set it is modeling. For data sets with evidence of mode or most likely value, it is recommended that triangular distributions be used. For small samples from which unrepresentative data points have been removed through rigorous analyses, uniform distributions are the preferred choice.

If distribution parameters are known, then the distribution is defined. For example, the normal distribution is defined by its mean and standard deviation. The uniform distribution is defined by its minimum and maximum values, while the triangular distribution is denoted by its minimum, most likely and maximum values. Generally, measures of dispersion—variance, standard deviation and P10-to-P90 range—show the extent to which a given data set spread around the mean (or P50, for a symmetric distribution).

Fig. 3.1 gives the three examples of input probability distributions.

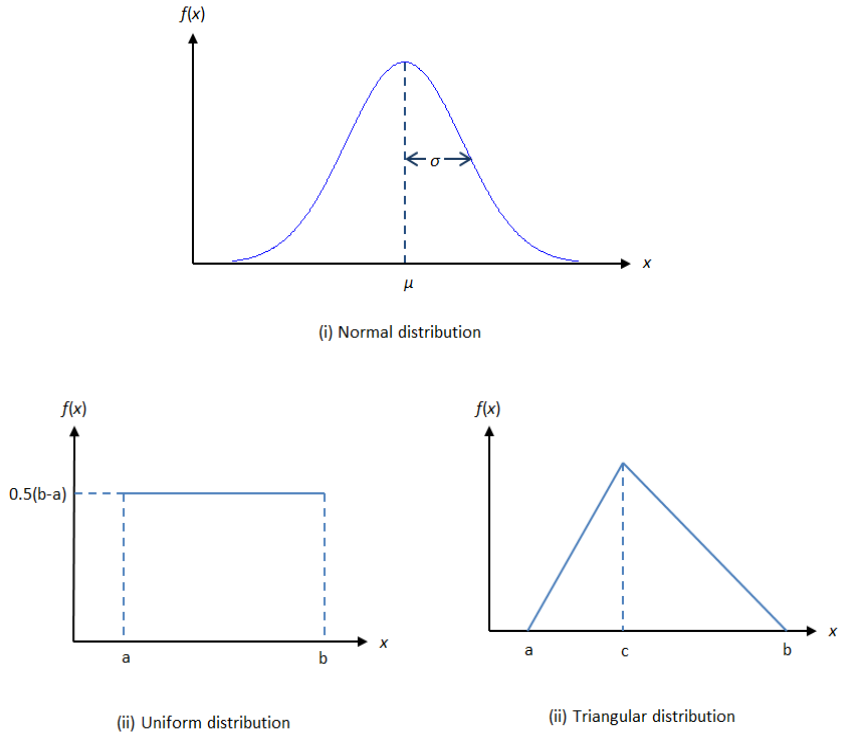

Figure 3.1—Different types of input probability distributions. The parameter, μ, is the mean; σ is the standard deviation; the minimum value is represented by a; b is the maximum value; and c is the most likely value. For a standard normal distribution, μ = zero, σ = 1.

3.4 Stochastic Model

The transformation of the deterministic models to stochastic models follows the procedure described in de Rocquigny et al. (2009). The input parameters are divided into two categories—uncertain inputs and fixed inputs. The input variables subject to randomness are treated as uncertain parameters, denoted by x. They are defined with appropriate probability distributions. Other variables with negligible degree of randomness, or inputs whose values are known with some certainty, are defined as fixed parameters and denoted by d. Both sets of input parameters are then applied in the preexisting deterministic model. After

several Monte Carlo trials, randomly distributed outputs denoted by Y are generated.
Eq. 3.1 is a generalized conceptual model for the stochastic modeling.

$$Y = G(x, d) \tag{3.1}$$

Fig. 3.2 gives a graphic representation of the Monte Carlo frame, with the preexisting model linking the output variables, Y, to a number of uncertain and fixed input parameters, x and d.

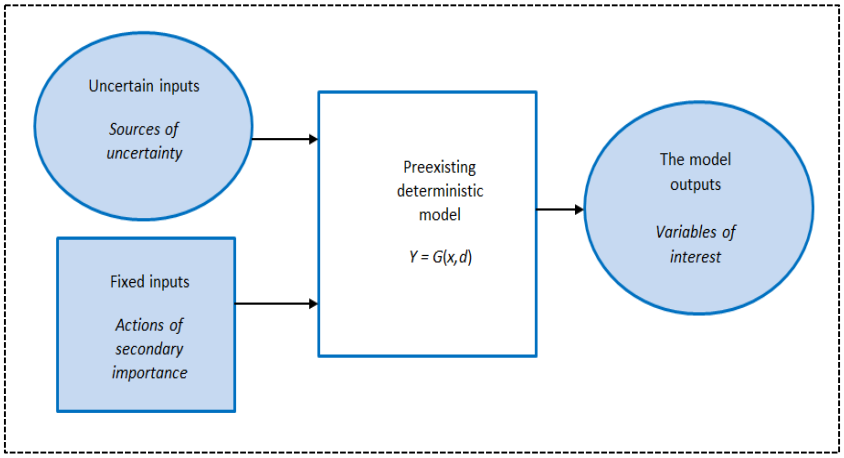

Figure 3.2—An idealized model for uncertainty propagation. The preexisting deterministic models form the bases of the uncertainty modeling.

4 Results and Discussion

The two example cases given in Chapter 2—UBD well planning and wellbore stability analyses—will be used to demonstrate the applications of the stochastic modeling.

The probability distributions used in the stochastic simulations are selected such that they are consistent with the range of input data they are modeling. The triangular distribution is represented by $T(a, c, b)$, the uniform distribution is represented by $U(a, b)$, and the normal distribution by $N(\mu, \sigma)$. Input uncertainties, which are expressed in percentages, quantitatively indicate how much the mean differ from the extremes values. However, they are only reasonable guesses based on field data and values quoted in the literature. There is also a room for further improvements.

4.1 Wellbore Stability Analyses

Reservoir engineers generally state that rocks are heterogeneous and anisotropic. Real rocks are difficult to describe because they are composed of non-perfect materials whose parameters are not easily known.

Geologic and petrophysical data used for WSA are known to be uncertain. They include in-situ horizontal stresses, overburden stress, pore pressure, cohesive rock strength, rock friction angle and so forth.

The stability models are not fully describing the physics of the subsurface phenomena. Thus, rock modeling can be best described as an ill-defined physical problem. The difference may be due to noise in measurements, measurement errors, and calibration. The input uncertainties may also be due to scarcity of data. There is a human error as well. This stems from the human imprecise knowledge of geologic systems and the data interpretation methods.

Uncertainty wellbore stability analyses have been discussed in previous studies (Morita 1995; Ottesen et al. 1999; Liang 2002; de Fontoura et al. 2002; Sheng et al. 2006; Aadnøy 2011). However, uncertainty propagation is yet to be addressed.

A fully probabilistic wellbore stability analysis is proposed in this work. The methodology has been discussed in detail in Paper III (Udegbunam et al.

2013a). The novel approach describes how uncertainty can be propagated from accessible input data to output variables.

The formation considered in the work is assumed homogeneous and isotropic. The model (Eq. 2.1), non-penetrating Kirsch solution for wellbore fracturing, and Mohr-Coulomb Shear-Failure Criterion for collapse (Eq. 2.2) are defined as the preexisting models for the stochastic WSA.

Fig. 4.1 presents a general procedure for stochastic wellbore stability analyses. The functions, $y = f(v, w, x)$ and $z = f(v, w)$, are the base models. The first step involves the random sampling of input variables. Then the random numbers are applied in the base models, to generate single-point outputs. This process is repeated for n times and the output histograms are constructed. If the output data are not realistic, the inputs are redefined or the models are calibrated against offset data.

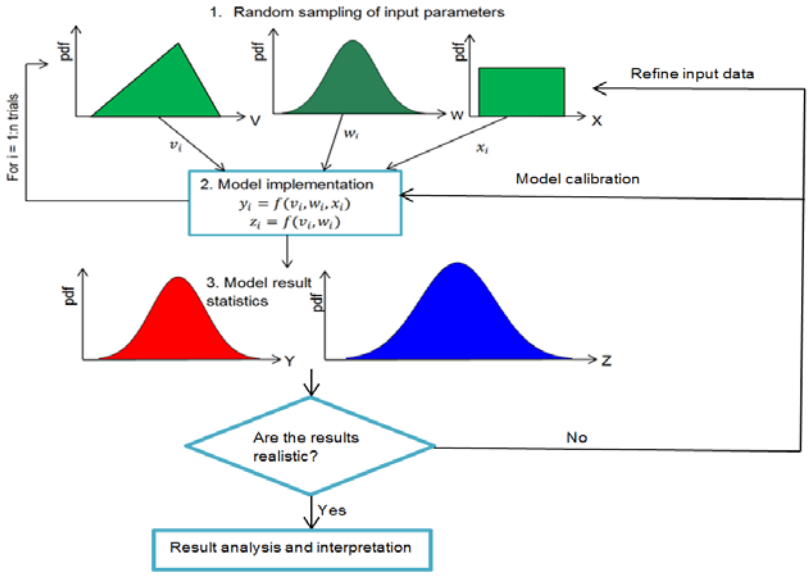

Figure 4.1—A schematic for general stochastic wellbore stability analyses.

4.1.1 Example Cases

Deterministic Prediction

Let σ_H = 1.8 sg; σ_h = 1.5 sg; P_o = 1.05 sg; α = 30°; τ_o = 0.5 sg.
Applying the input data in Eqs. 2.1 and 2.2, the wellbore fracture gradient is 1.65 sg, and the collapse gradient is 1.07 sg.
In this case, the single-point estimates of the geopressures will give too optimistic a drilling window. This may lead to drilling problems. However, it is impossible to assess the associated risk and uncertainty based on these fixed input data. The only way to achieve this is by running stochastic simulations.

Stochastic Prediction

Case A. Table 4.1 presents the input parameters (now random variables) with assumed uncertainties. All the inputs are assigned a triangular distribution, as shown in **Table 4.2**.

TABLE 4.1—INPUT PARAMETERS TREATED AS RANDOM VARIABLES

Input Parameter	Most Likely Value	Uncertainty in Estimation (± %)	Range of Magnitude
σ_H	1.8 sg	10	1.62 – 1.98 sg
σ_h	1.5 sg	5	1.43 – 1.58 sg
P_o	1.05 sg	30	0.74 – 1.37 sg
α	30°	20	24° – 36°
τ_o	0.5 sg	50	0.25 – 0.75 sg

TABLE 4.2—INPUT DISTRIBUTIONS

Input Parameter	Probability Distribution
σ_H (sg)	$\sigma_H = T$ (1.62,1.8,1.98)
σ_h (sg)	$\sigma_h = T$ (1.43,1.5,1.58)
P_o (sg)	$P_o = T$ (0.74,1.05,1.37)
α (rad)	$\alpha = T$ (0.420,0.524,0.628)
τ_o (sg)	$\tau_o = T$ (0.25,0.5,0.75)

The input distributions are applied in the deterministic stability models. After 600,000 Monte Carlo trials, the fracture and collapse pressure distributions are generated. The simulation time is approximately 46 s.
Fig. 4.2 gives the geopressure distributions.

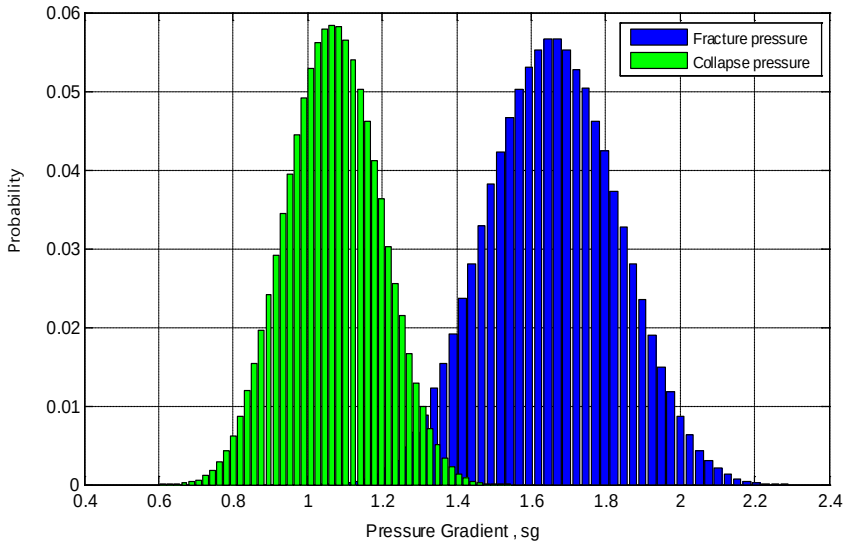

Figure 4.2—Fracture and collapse pressure distributions. Number of Monte Carlo trials = 600,000.

Now the exact solutions become probability distributions. The probabilistic models offer the means for the input uncertainty propagations. With this, a better confidence levels can be defined based on the output variances.
However, there is crossing of the stability curves as show in **Fig. 4.2**. It means that the same well pressure will initiate wellbore fracturing and collapse. The unphysical situation is not evident from the deterministic analyses.
The critical fracture pressure must exceed the critical collapse pressure by a stability margin, δ, (Aadnøy and Hansen 2005). For a more realistic scenario, the input distributions are redefined by imposing the stress bounds described in Aadnøy and Hansen (2005). In real situation, this may also involve rigorous data analysis and calibration study.

Case B. Table 4.3 gives the stress bounds for the three types of in-situ stress state described in Anderson (2012). Here, a normal fault stress state is assumed, based on the magnitudes of the stress data.

Table 4.4 gives the redefined input-parameter distributions.

The stochastic simulations are repeated with the redefined input distributions.

Fig. 4.3 presents the resulting fracture and collapse pressure distributions after running 600,000 Monte Carlo trials.

TABLE 4.3—IN-SITU STRESS BOUNDS FOR BOREHOLES IN THE THREE PRINCIPAL STRESS DIRECTIONS

Stress State	Bound 1	Bound 2	Bound 3
Normal fault	$\sigma_h A \geq \sigma_H B + C$	$\sigma_H A \geq \sigma_v B + C$	$\sigma_h A \geq \sigma_v B + C$
Strike-slip fault	$\sigma_h A \geq \sigma_H B + C$	$\sigma_v A \geq \sigma_H B + C$	$\sigma_h A \geq \sigma_v B + C$
Reverse fault	$\sigma_h A \geq \sigma_H B + C$	$\sigma_v A \geq \sigma_H B + C$	$\sigma_v A \geq \sigma_h B + C$

$A = 7 - \sin\alpha$, $B = 5 - 3\sin\alpha$, $C = P_o (1+\sin\alpha) + 2(\delta - \tau_o \cos\alpha)$.

TABLE 4.4—REDEFINED INPUT DISTRIBUTIONS

Input Parameter	Probability Distribution
σ_H (sg)	$\sigma_H = T$ (1.93,1.97,2.0)
σ_h (sg)	$\sigma_h = T$ (1.75,1.78,1.8)
P_o (sg)	$P_o = T$ (1.45,1.5,1.55)
α (rad)	$\alpha = T$ (0.349,0.436,0.524)
τ_o (sg)	$\tau_o = T$ (0.25,0.38,0.5)

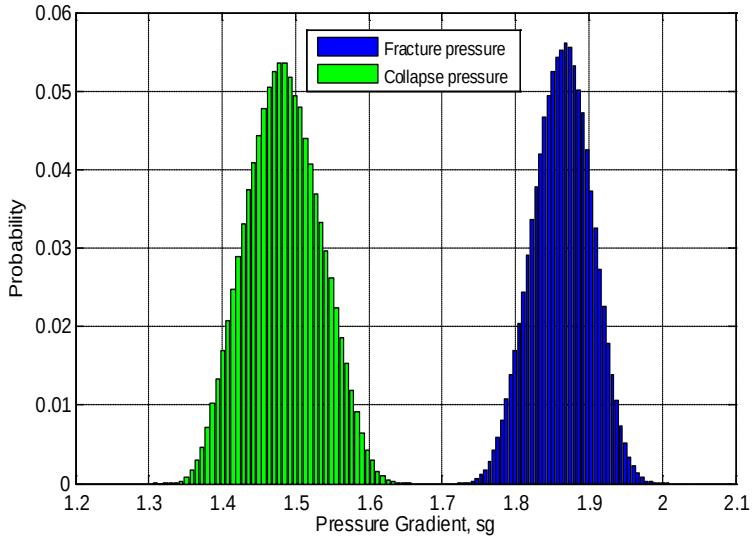

Figure 4.3—Fracture and collapse pressure distributions. Number of Monte Carlo trials = 600,000.

There is no crossing of the stability curves this time. Therefore, the stochastic models have predicted solutions that are more realistic.

Tables 4.5 and 4.6 compare the cumulative uncertainties in the stochastic geopressure prognoses for the Cases A and B respectively.

TABLE 4.5—UNCERTAINTY IN THE PRESSURE PREDICTION

	Pressure	
Data Statistics	Fracture	Collapse
P10 (sg)	1.43	0.91
P50 (sg)	1.66	1.07
P90 (sg)	1.88	1.23
Mean (sg)	1.66	1.07
Standard deviation (sg)	0.174	0.123
Cumulative uncertainty (%)	±38	-44/+45

Cumulative uncertainty = (max/min value – expected value)/expected value

TABLE 4.6—UNCERTAINTY IN THE PRESSURE PREDICTION

	Pressure	
Data Statistics	Fracture	Collapse
P10 (sg)	1.81	1.42
P50 (sg)	1.86	1.48
P90 (sg)	1.91	1.55
Mean (sg)	1.86	1.48
Standard deviation (sg)	0.0397	0.0503
Cumulative Uncertainty (%)	±8	±12

Cumulative uncertainty = (max/min value – expected value)/expected value

In either case, the cumulative uncertainty in the collapse-pressure prognosis exceeds that of the fracture pressure. However, the Case B (Table 4.6) shows improved results compared with the Case A (Table 4.5). For example, the cumulative uncertainty in the fracture-pressure prediction is reduced by a factor of 0.79 (that is, from ±38 to ±8%).

4.1.2 Stochastic Sensitivity Analysis

The purpose of sensitivity analysis is to investigate how models respond to the variations in the random inputs. Generally, the input parameters are ranked according to their relative importance. In this way, the inputs that require further research to improve the knowledge base are determined. As expressed in Saltelli et al. (2008), one can then justify that the input data are accurate enough for a model to give reliable predictions. If large discrepancies exist in the data, more work will be directed towards improving the estimations of these uncertain parameters. The results of the analysis will be invaluable during the model calibration study.

The goal here is to determine the input parameters that mainly contribute to the cumulative uncertainties in the critical fracturing and collapse pressure predictions. In the analyses, the same Monte Carlo method is followed, except that only the input under study is treated as a random parameter. The scenario in which all the inputs are uncertain is also included for comparison.

Table 4.7 presents the input data used for the sensitivity analyses.

Table 4.8 gives different combinations of the input parameters for the test cases.

TABLE 4.7—INPUT PARAMETERS FOR MONTE CARLO SENSITIVITY ANALYSES

Input Parameter	Input Distributions	Most Likely Value
σ_H (sg)	$\sigma_H = T$ (1.93,1.97,2.0)	1.97
σ_h (sg)	$\sigma_h = T$ (1.75,1.78,1.8)	1.78
P_o (sg)	$P_o = T$ (1.45,1.5,1.55)	1.50
α (rad)	$\alpha = T$ (0.349,0.436,0.524)	0.436
τ_o (sg)	$\tau_o = T$ (0.25,0.38,0.5)	0.38

TABLE 4.8—DIFFERENT COMBINATIONS OF INPUTS FOR THE SENSITIVITY ANALYSES

Fracture Pressure				Collapse Pressure					
	Uncertain Input				Uncertain Input				
Case	σ_H	σ_h	P_o	Case	σ_H	σ_h	P_o	τ_o	α
Base Case	Y	Y	Y	Base Case	Y	Y	Y	Y	Y
Case 1	Y	N	N	Case 1	Y	N	N	N	N
Case 2	N	Y	N	Case 2	N	Y	N	N	N
Case 3	N	N	Y	Case 3	N	N	Y	N	N
				Case 4	N	N	N	Y	N
				Case 5	N	N	N	N	Y
Y = Yes, N = No									

Fig 4.4 shows the plots of the geopressure distributions for the cases.

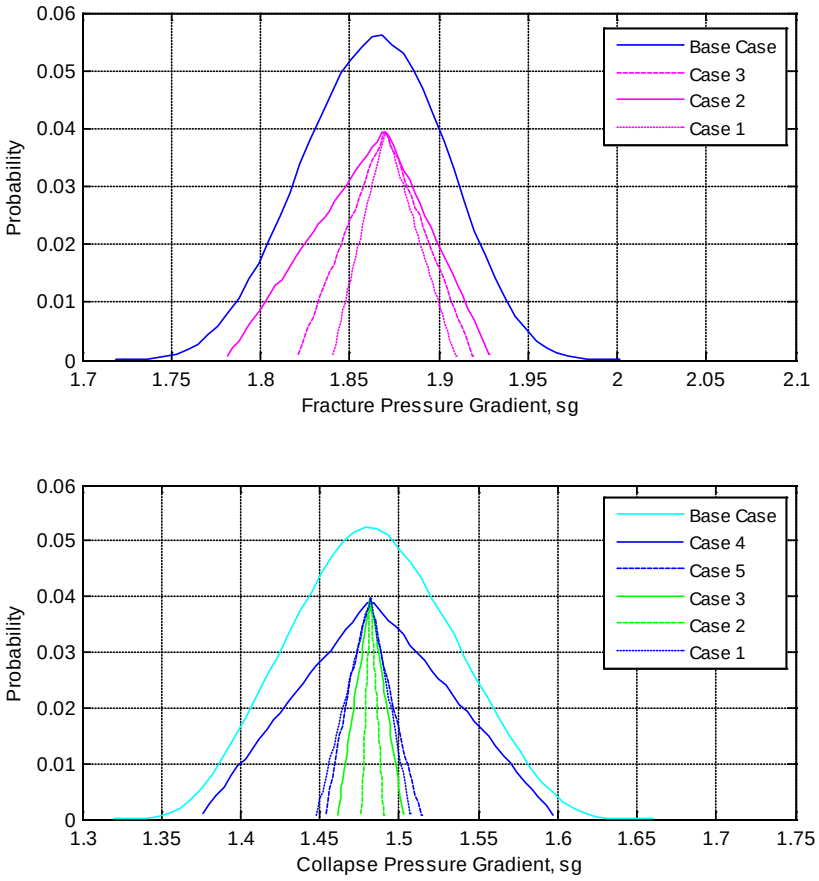

Figure 4.4—Monte Carlo sensitivity Analyses. The plots show the pressure distributions for different cases. Top: fracture pressure; Bottom: collapse pressure.

From **Fig. 4.4** (Top), the Case 2 is the fracture pressure distribution when the only uncertain input is the minimum horizontal stress. This distribution has the highest data spread compared with the Cases 1 and 3. Therefore, the minimum horizontal stress is the most significant input parameter responsible for the variability in the critical fracture pressure prediction (Base Case). The second most influential parameter is the pore pressure (Case 3).

For the collapse pressure, the cohesive rock strength (Case 4) proves to be the most influential parameter in the critical collapse pressure prognosis. This is

expected because a sedimentary rock can be highly consolidated in some places, and unconsolidated with zero cohesive strength nearby. Previously, Morita (1995) observed that the rock strength is the most important parameter in the collapse pressure estimation, for both shale and sand formations.
The pressure distribution for the Case 2 has the least spread compared with the Cases 1, 3, and 5. Thus, the minimum horizontal stress is the parameter of least importance.

4.2 Underbalanced Operations

4.2.1 Uncertainty BHP Prediction

The uncertainty modeling of underbalanced operations has been discussed in Udegbunam et al. (2013b). From literature (Lage 2000), the two-phase flow model for predicting the downhole pressure is associated with uncertainties. The uncertainties may result from the input-parameter uncertainties and uncertainty related to the modeling process.

This section presents a simple stochastic approach for working out the UBD operational window. In contrast with the deterministic prediction, here the annular BHP follows a probability distribution.
A vertical well is considered. For simplicity, the drill string consists of a drill pipe whose outer diameter is 3.5 in. There is no BHA.
The two-phase flow system consists of liquid and gas. Both are injected co-currently into the annulus via the drill pipe. Temperature effects are neglected because the steady-state flow model (Section 2.3.1) is formulated under isothermal condition and with simple closure laws. This ideal condition is not true for real downhole conditions, where multiphase properties such as density and viscosity vary with the wellbore temperature. The assumption, however, by no means negates the essence of the stochastic modeling—the research focus.
The well and fluid properties are listed below.

- Well depth = 2000 m
- Annulus: outer diameter, d_o, = 6.3 in (0.16 m); inner diameter, d_i, = 3.5 in (0.089 m)

- Fluid-injection rates: liquid rate = 1400 L/min (0.0233 m^3/s); gas rate ranges from zero to 60 m^3/min (1 m^3/s)
- Liquid viscosity, μ_l, = 1 cp (0.001 Pa.s); gas viscosity, μ_g = 0.01 cp (0.00001 Pa.s)
- The liquid and gas volume rates are measured at standard surface conditions.
- The reservoir fluid is a gas with the same properties as the injected gas. The average productivity index, PI, is 2.83E-08 $m^3/s/Pa$.

Uncertain Input Parameters. Some of the model input parameters that are subject to randomness include gas-slip parameters, C_0 and V_d, parameter related to friction factor calculation, f_c, pore pressure, P_o, and collapse pressure, P_{coll}. There are also uncertainties associated with choke operability and reservoir fluid influx. They are implemented with parameters P_{cho} and PI. Other inputs are considered fixed parameters.
The parameter, f_c, is included in Eq. 2.10 as:

$$\frac{\Delta \overset{*}{P}_f}{\Delta z} = f_c \frac{\Delta P_f}{\Delta z} \tag{4.1}$$

In general, the distributions should be chosen such that they reflect the physics of the problem. The focus here is to demonstrate a stochastic methodology for the UBD well planning. Investigating the goodness of fit of the input distributions will be a discussion for future work.
Triangular distributions are assigned to the gas-slip parameters and f_c. As indicated in Adams et al. (1993) and Nilsen et al. (2001), all pressure parameters are modeled with normal distributions.
Table 4.9 presents the random inputs with their assumed uncertainties and probability distributions.

TABLE 4.9—UNCERTAIN INPUT PARAMETERS AND THEIR PROBABILITY DISTRIBUTIONS

Parameter	Fixed value	Uncertainty (%)	Type of distribution
C_0	1.20	-17/+2	$C_0 = T$ (1,1.2,1.22)
V_d	0.50	-30/+10	$V_d = T$ (0.35,0.50,0.55)
f_c	1	± 10	$f_c = T$ (0.9,1,1.1)
P_{cho}	6	± 33	$P_{cho} = N$ (6,0.817)
PI	244.50	-58/+50	$PI = N$ (244.5,70.3)
P_o	200	± 10	$P_o = N$ (200,8.17)
P_{coll}	160	± 8	$P_{coll} = N$ (160,5.31)

T = triangrnd, N = normrnd. All pressures are given in bar; PI is in m^3/day/day; V_d is in m/s; C_0 and f_c are dimensionless.

All simulations are run in MATLAB. First, the deterministic BHP prediction will be presented as a base case. In this scenario, the fixed values of the input parameters are used in the simulations.

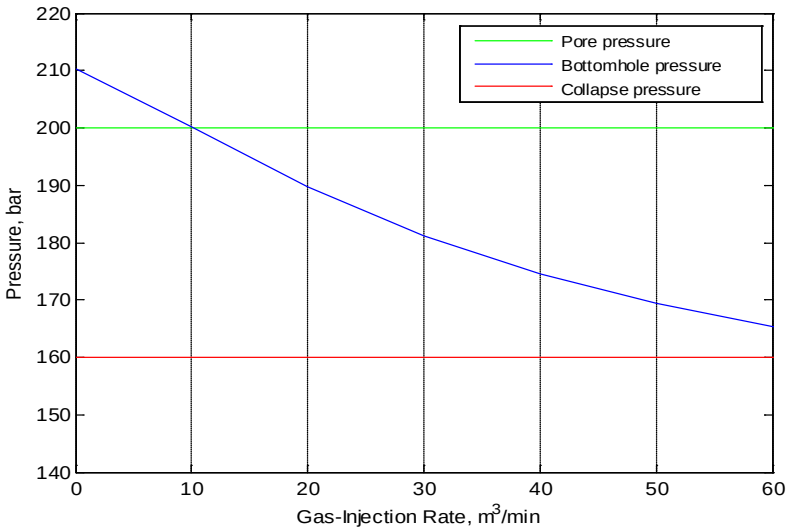

Figure 4.5—Annular bottomhole pressure versus gas-injection rates. Liquid rate = 1400 L/min.

Fig 4.5 shows that the predicted BHP falls within the UBD operational window for the injection-gas rate greater than 10 m^3/min. During unloading, the BHP decreases due to the decrease in the mixture density of the multiphase fluids. The well friction builds up as GVF increases. The system, according to Saponja (1998), may eventually reach an optimum point where the reduced hydrostatic

pressure is balanced by increased annular friction. This optimal circulating point is the minimum achievable BHP for the specified liquid rate.

Judging from the figure, one may be at risk to conclude that there is no possibility of wellbore collapse. This is a major drawback in relying only on the deterministic results when selecting the operational parameters.
Stochastic simulations can be used to gain more insights, considering the modeling uncertainties and extreme dynamics of the multiphase system.

Stochastic Results. The uncertain and fixed inputs are applied in the Monte Carlo frame described in **Fig. 3.2**, with the deterministic model as the basis. For each gas-injection rate, the stochastic model predicts BHP that follows a probability distribution. The criterion for convergence of the results is by visual inspection. After repeating 100,000 Monte Carlo trials for several times, the resulting histograms appear nearly identical. This number is good enough for convergence in the present case. For a more complex hydraulic model, the Cramér-von Mises Criterion described in Anderson (1962) can be used as a measure for testing the result convergence.
The P10, P50, and P10 of the BHP distribution are plotted against the gas-injection rate. The results are the three BHP bands—the lower limit, the most likely, and the upper limit—presented in **Fig. 4.6**. It takes approximately 11 hours to run the entire simulations.

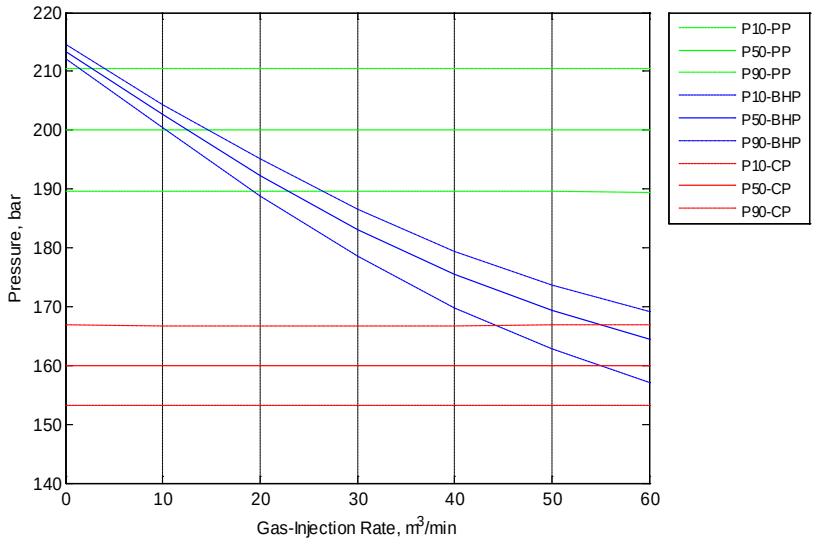

Figure 4.6—Annular BHP distributions at different gas-injection rates. Liquid rate = 1400 L/min; number of Monte Carlo trials = 100,000; PP = pore pressure; CP = collapse pressure.

Fig. 4.6 shows that uncertainty in the prediction of the BHP increases with the annular gas volume. This effect is not evident from the deterministic results. In addition, the UBD operating window is further limited by the extreme values of the pore and collapse pressures, that is, P10-PP and P90-CP bands. The probabilistic results indicate that some BHP values fall outside this window. Again, this is not the case with the deterministic prediction.

To maintain an underbalanced mode, considering the wellbore stability, the gas-injection rates in the range of 30–40 m^3/s is recommended for this case. This shows that a probabilistic approach can give a different recommendation—regarding the UBD operational window—from a pure deterministic method. While selecting the optimum gas-injection rate, it is also important that cutting transport and downhole motor requirements be taken into consideration.

Overbalance and Collapse Detections. The deterministic flow model lacks the capability to predict the likelihood of overbalance or collapse condition. By contrast, the stochastic model can predict the chance of the BHP exceeding the

UBD operating limits. During the simulation, the numerical counter records the number of times there is a pressure overbalance or collapse condition. In the end, the ratio of this number to the number of Monte Carlo trials gives the probability of overbalance or collapse.

This can be demonstrated with the three gas-injection gas rates—15, 30, and 40 m^3/min. The number of Monte Carlo trials is 100,000.

Figs. 4.7 through 4.9 present the results of the simulations.

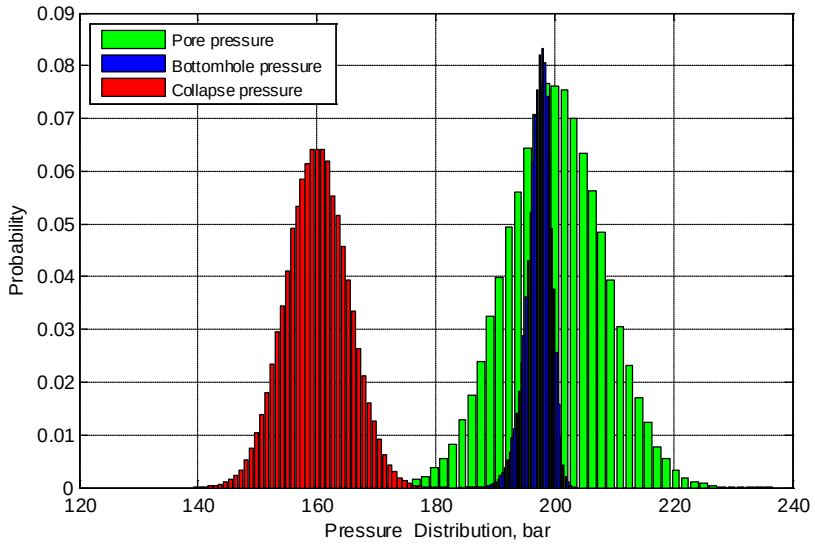

Fig. 4.7—Overbalance and collapse detections. Gas-injection rate = 15 m^3/min, liquid rate = 1400 L/min. Probability: overbalance = 0.4097, collapse = zero.

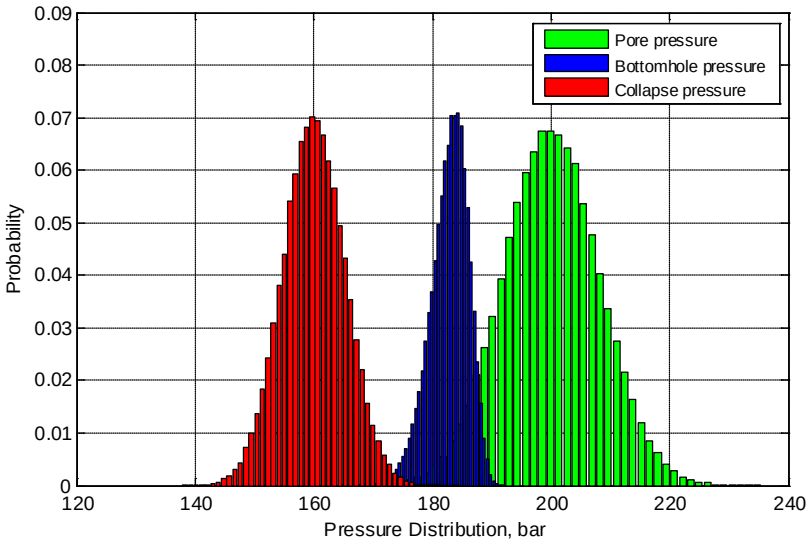

Fig. 4.8—Overbalance and collapse detections. Gas-injection rate = 30 m^3/min, liquid rate = 1400 L/min. Probability: overbalance = 0.0393, collapse = 0.0002.

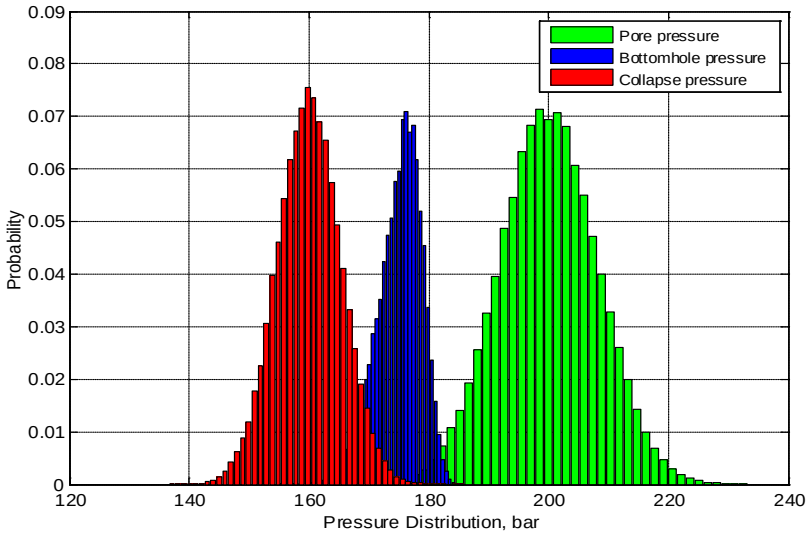

Fig. 4.9—Overbalance and collapse detections. Gas-injection rate = 40 m^3/min, liquid rate = 1400 L/min. Probability: overbalance = 0.0049, collapse = 0.0134.

Fig. 4.7 shows that the chance of having pressure overbalance is high at lower gas rates, as indicated by the probability. This likelihood decreases as the gas-injection rate is doubled (**Fig 4.8**).
By contrast, the probability of collapse increases as more gas is pumped into the annulus. There is a higher chance of having wellbore collapse when the gas-injection rate is 40 m^3/s (**Fig. 4.9**), compared with the zero probability when the gas-injection rate is 15 m^3/s.
Table 4.10 presents a summary of the simulation results.

TABLE 4.10—OVERBALANCE AND COLLAPSE DETECTIONS

	Probability (%)	
Gas-Injection Rate (m^3/min)	Overbalance	Collapse
15	40.97	0
30	3.93	0.02
40	0.49	1.34

The probabilistic approach not only provides a means for the uncertainty propagation, it also ensures that the annular well pressure remains underbalanced in the target section.

4.2.2 Mechanics of Collapse for UBD

Boundary value problems will be used to show how the wellbore collapse may be induced during underbalanced drilling.

Overbalance (OB)

For a conventional overbalanced drilling, $P_o < P_w$. Eq. 2.2 defines the critical well pressure that will cause wellbore collapse as:

$$P_{wc} = \frac{1}{2}(3\sigma_H - \sigma_h)(1 - \sin\alpha) + P_o \sin\alpha - \tau_o \cos\alpha$$

Eq. 2.2 is true for both permeable and impermeable rocks.

Underbalance (UB)

Permeable Rocks. In underbalanced drilling, $P_o > P_w$. For permeable rocks such as sandstones and carbonates, the formation fluid will flow into the wellbore when $P_w = P_o$.
Let $P_w = P_o$. Replacing P_o with P_w, that is P_{wc}, in the collapse model (Eq. 2.2), the resulting equation is given by Eq. 4.2. The equation gives the critical well pressure that will initiate wellbore collapse during underbalanced operations.

$$P_{(UBD)wc} = \frac{\frac{1}{2}(3\sigma_H - \sigma_h)(1-\sin\alpha) - \tau_o \cos\alpha}{1-\sin\alpha} \tag{4.2}$$

During UBD, the reservoir flow will stabilize the wellbore at $P_w = P_{(UBD)wc}$.
If the well pressure falls under the critical value, the collapse of the wellbore wall initiates and eventually causes its failure (Aadnøy and Reza 2010).

Impermeable Rocks. Impervious rocks like shales may not allow inward flow of the formation fluid into the wellbore, even if the well pressure is less than the pore pressure. Therefore, Eq. 2.2 defines the critical well pressure that will cause wellbore collapse in this situation.

Figs. 4.10 and 4.11 respectively give the boundary conditions for wellbore collapse, for permeable and impermeable rocks. The figures also indicate the reservoir conditions for conventional drilling and UBD.

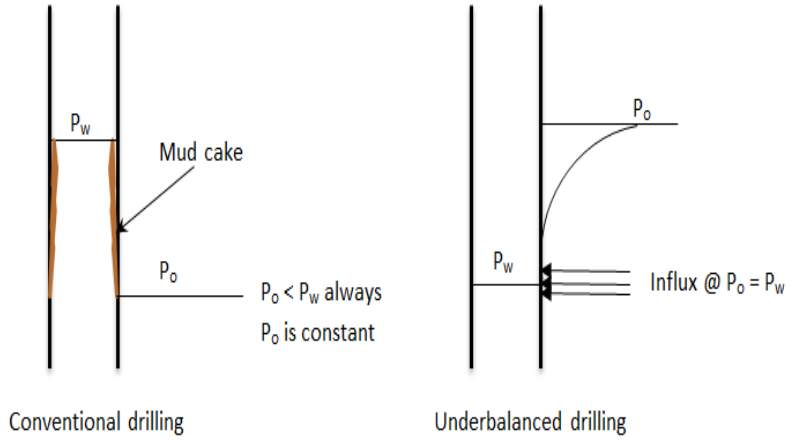

Figure 4.10—Boundary conditions for wellbore collapse, for permeable rocks such as sandstones and carbonates.

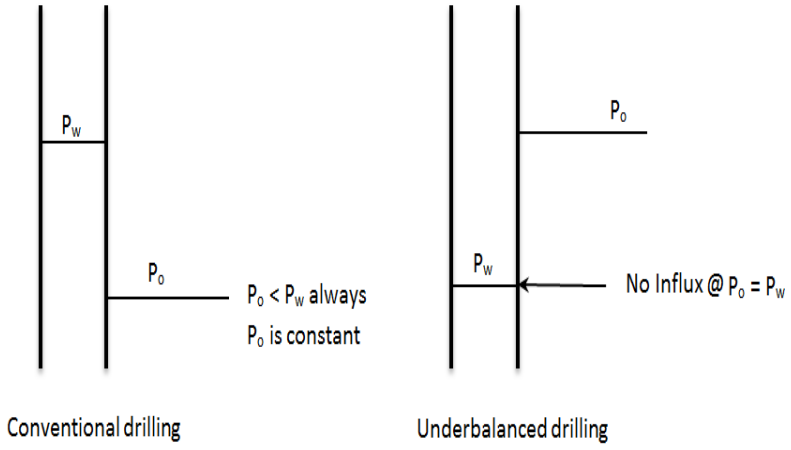

Figure 4.11—Boundary conditions for wellbore collapse, for impermeable rocks like shales.

Table 4.11 summarizes the implementation of the collapse model.

TABLE 4.11—IMPLEMENTATION OF THE COLLAPSE MODEL

Rock	Boundary Condition	Collapse Model
Permeable		
OB	Non-penetrating	Eq. 2.2
UB	Penetrating	Eq. 4.2
Impermeable		
OB	Non-penetrating	Eq. 2.2
UB	Non-penetrating	Eq. 2.2

4.2.3 Sensitivity Analysis for UBO

The main purpose of the sensitivity analysis is to determine which input parameters largely influence the BHP prediction. Here, only flow-dependent parameters, C_0, V_d, and f_c, are considered uncertain. For the base case, all the inputs are uncertain, and their probability distributions are used in the simulation. The deterministic scenario where the values of the parameters remain unvaried is also included.

The probability distribution of the input variable under investigation and the fixed values of other inputs are applied in the Monte Carlo frame. The BHP histogram is generated after 100,000 Monte Carlo trials.

Fig 4.12 is derived by plotting the P50 values of the resulting BHP distributions against the gas-injection rates.

Table 4.12 presents different combinations of the input parameters for the simulations.

TABLE 4.12—DIFFERENT COMBINATIONS OF INPUT PARAMETERS FOR THE SENSITIVITY ANALYSIS

	Input Parameter		
Case	C_0	V_d	f_c
Base case	$C_0 = T(1.01,1.2,1.22)$	$V_d = T(0.35,0.5,0.55)$	$f_c = T(0.9,1.0,1.1)$
BHP-C_0	$C_0 = T(1.01,1.2,1.22)$	0.50	1.0
BHP-V_d	1.20	$V_d = T(0.35,0.5,0.55)$	1.0
BHP-f_c	1.20	0.50	$f_c = T(0.9,1.0,1.1)$
Det case	1.20	0.50	1.0
PI = 244.5 m^3/day/bar; P_o = 200 bar; P_{coll} = 160 bar; P_{cho} (surface backpressure) = 6 bar			

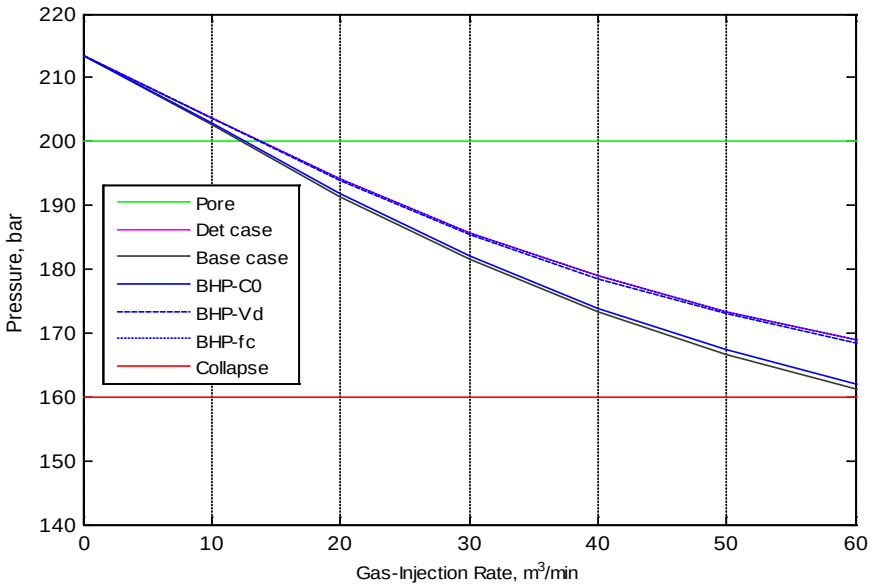

Figure 4.12—Sensitivity analysis. Each plot of the annular pressure versus gas rates depicts the contribution of the respective input to the uncertainty in the BHP prediction.

From the plots above, it can be seen that the BHP-f_c profile overlaps with the deterministic case (Det case). This clearly shows that f_c is the least significant input parameter in this simulation scenario. The BHP-V_d profile nearly approximates the Det case. Hence, the gas drift velocity relative to the liquid is the second least significant input.

On the contrary, BHP-C_0 profile approaches the Base case. Therefore, C_0 is the most influential input parameter largely responsible for the cumulative uncertainty in the BHP prediction.

The UBD multiphase circulating system represents a highly dynamic flow situation. Because the values of C_0 and V_d depend on the prevailing two-phase flow pattern, it is pertinent that comprehensive mechanistic models (Lage and Time 2000) be included in future studies. This also requires the use of more realistic closure laws and inclusion of wellbore temperature effects. A similar sensitivity analysis can then be carried out, to determine the most dominating parameters with respect to the uncertainty in the BHP.

5 A Transient Model for Well Flows

5.1 Introduction

Hybrid flux-splitting schemes for solving the compressible Euler and Navier-Stokes equations are a new development in upwind schemes. The schemes combine the efficiency of flux-vector splitting (FVS) schemes and the accuracy of flux-difference splitting schemes (Evje and Fjelde 2003). An example of such schemes is the Advection Upstream Splitting Method (AUSM) described in Liou and Steffen (1993). Liou (1996) extended the AUSM scheme to AUSM$^+$.
The attractive attributes of AUSM in comparison with other upwind schemes are accuracy, efficiency and robustness. The AUSM$^+$ scheme has demonstrated that it can produce exact resolution of contact and shock discontinuities and preserve positivity property of some primitive variables. It can also be easily extended to other hyperbolic systems due to its simplicity.

Based on the AUSM, Evje and Fjelde (2003) proposed a hybrid scheme termed 'AUSMV' that can be used to solve a hyperbolic system of conservation laws. The two-phase model was a sequel to the scheme proposed in Evje and Fjelde (2002). The model has a generic form:

$$\partial_t W + \partial_x F(x,W) = G(x,W) \tag{5.1}$$

where W represents the conservative variables, F is flux, G is a source term, x is the coordinate along the flow direction, and t is time.

Solving such hyperbolic model with classical schemes such as Godunov-type schemes (Harten 1983; Osher 1984) and Roe-type schemes (Roe 1980; Roe 1981) is quite difficult. This is because the schemes require analytical calculation of the Jacobian of the flux function. The alternative schemes proposed in Masella et al. (1999) and Romate (1998) have some drawbacks. The Jacobian calculation is time-consuming because it is based on the conservative variables.
The AUSMV scheme combines AUSM and FVS scheme (a van Leer scheme) in an appropriate way. This approach eliminates the need for algebraic manipulation of the Jacobian and reduces the numerical computational time. The scheme, according to Evje and Fjelde (2003), also gives low numerical dissipation at volume-fraction contact discontinuities and is able to produce stable and non-oscillatory solutions.

5.2 The AUSMV Scheme

The one-dimensional, two-phase model is based on the drift-flux formulation. The scheme consists of two mass conservation laws (one for each phase) and a conservation law for mixture momentum. This construct reduces the two momentum equations in the two-fluid model to one, hence eliminating the associated mathematical complications. A coupling between the phase velocity fields is achieved with the slip relation proposed by Zuber and Findlay (1965). The model is formulated under isothermal conditions and with simple closure relations. The ideal condition, however, is in contrast with a real downhole situation—where wellbore temperature affects the multiphase physical properties such as density and viscosity. Future works will include thermal effects. This can be implemented by assuming a constant temperature gradient along a wellbore or by combining the two-phase model with a model for radial and vertical heat transfer (Rommetveit et al. 2003).
Eqs. 5.2 through 5.4 give a system of the hyperbolic laws—two mass conservation laws (for liquid and gas) and one conservation law for mixture momentum.

$$\frac{\partial}{\partial t}(\alpha_l \rho_l) + \frac{\partial}{\partial x}(\alpha_l \rho_l v_l) = \Gamma_l \tag{5.2}$$

$$\frac{\partial}{\partial t}(\alpha_g \rho_g) + \frac{\partial}{\partial x}(\alpha_g \rho_g v_g) = \Gamma_g \tag{5.3}$$

$$\frac{\partial}{\partial t}(\alpha_l \rho_l v_l + \alpha_g \rho_g v_g) + \frac{\partial}{\partial x}(\alpha_l \rho_l v_l^2 + \alpha_g \rho_g v_g^2 + p) = -q \tag{5.4}$$

The unknowns are the liquid and gas densities (ρ_l, ρ_g), the phase volume fractions (α_l, α_g), the phase velocities (v_l, v_g), and well pressure, p.
Assuming that there is no mass exchange between the liquid and gas, the phase mass transfer coefficients, Γ_l and Γ_g, become zero.

However, the main contribution of the present work to the AUSMV development is the extension of the scheme to MPD and UBD applications. The effect of numerical diffusion is also demonstrated, including a suggestion on how to improve the accuracy of the scheme.
For a detailed discussion on the properties of the scheme and discretization procedure, readers are recommended to see Paper V (Udegbunam 2014). The concern here is to show that the AUSMV scheme can handle dynamic processes often encountered in well operations. Such well transients include effect of

reservoir fluid influx, unloading, and connection. This will be illustrated with DGD and UBD example cases.

5.3 Dual-Gradient Drilling

The dual-gradient system studied in this work is similar to the system described in Falk et al. (2011) and Fossli and Sangesland (2006). With the technique, well pressure can be managed during drilling by adjusting the mud level in a marine riser. Handal (2011) also did an extensive numerical work on this floating mud-cap system. In this section, the aim is to demonstrate that the AUSMV scheme can also handle the flow dynamics associated with the MPD system. This work investigates the effects of kick, flow area change, and numerical discretization on annular BHP development.

Wellbore and Fluid Data. The vertical well considered in this example is 2000 m deep. The drill string consists of a drill pipe whose outer diameter is 5" (0.127 m). There is no BHA. The inner annular diameter is 8 ½" (0.216 m).
The marine riser is 1000 m long, with an inner diameter of 20" (0.508 m). Thus, an area discontinuity is expected because different flow areas will exist between the drill pipe and riser and between the drill pipe and the annulus.
The liquid sonic velocity, a_l = 1500 m/s, and viscosity, $\mu_l = 5\times10^{-2}$ Pa.s. The reservoir fluid is a gas with viscosity, $\mu_g = 5\times10^{-6}$ Pa.s and the sonic velocity, a_g = 316 m/s. The gas-slip parameters, C_0 = 1.1 and V_d = 0.5 m/s. The fluid densities vary with the well pressure. All fluid volumes are measured at standard surface conditions.

Effect of Gas Kick. The kick volumes considered in the numerical simulations are 0.5 and 1 m^3. At the onset, the liquid-injection rate is 600 L/min. From 300 to 790 s, the mud level in the riser is gradually lowered at the suction rate of 4500 L/min. The reservoir gas flows into the well between 1000 and 1070 s. At 1100 s, the kick is circulated out of the well with a suction rate of 600 L/min. This ensures that the volume of the drilling fluid in the annulus is maintained.
Fig 5.1 represents a simplified well for the DGD system.

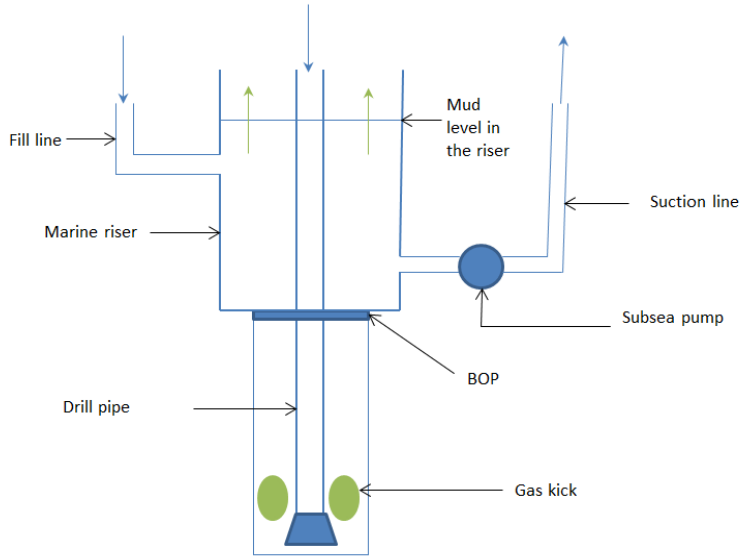

Figure 5.1—A simplified well for the DGD system. The kick migrates upward and is separated in the riser

Fig. 5.2 presents annular BHP development with time, for the two kick volumes.

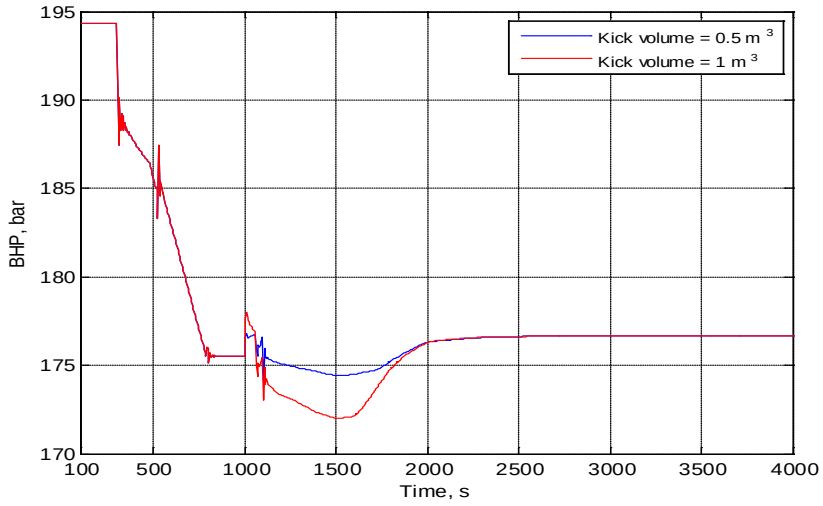

Figure 5.2—Annular bottomhole pressure versus time. Number of cells = 25.

The figure shows that there is a sudden increase in the annular BHP at 1000 s, when the gas enters the well. This is probably due to increase in the well friction. It is also observed that the pressure decreases, and then increases, before it stabilizes after 2500 s. The effect of the gas kick on the BHP in the well is noticeable due to area-to-volume effect. The kick will have a lower area-to-volume ratio in the well than in the riser, but the mud-level increase in the riser will correspond to the kick volume. Thus, the height of the kick is larger in the well than when it enters the riser with a larger flow area.

Though the well pressure profiles presented in **Fig. 5.2** exhibit similar trend, the pressure drop for 1 m^3 kick is larger. This is because the area-to-volume effect becomes more pronounced as the kick volume becomes larger. The well, however, is under static conditions when taking the kick in each case.

In addition, the BHPs at 1000 s and at the end of the simulation are the same for the two cases. This is because the mass of drilling fluid is conserved.

Figs. 5.3a through 5.3c present snapshots of the gas kick at different time intervals, as it migrates up the well.

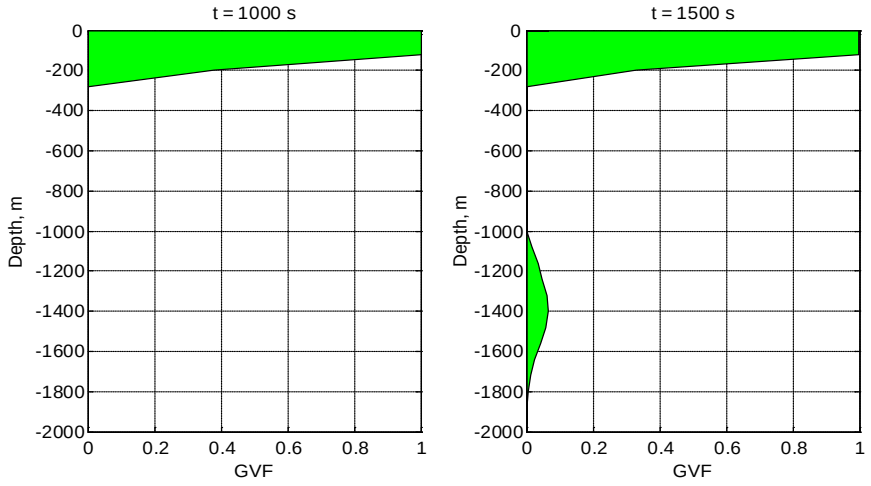

Figure 5.3a—Depth versus gas volume fraction at t = 1000 s and t = 1500 s. Kick volume = 0.5 m^3, number of cells = 25.

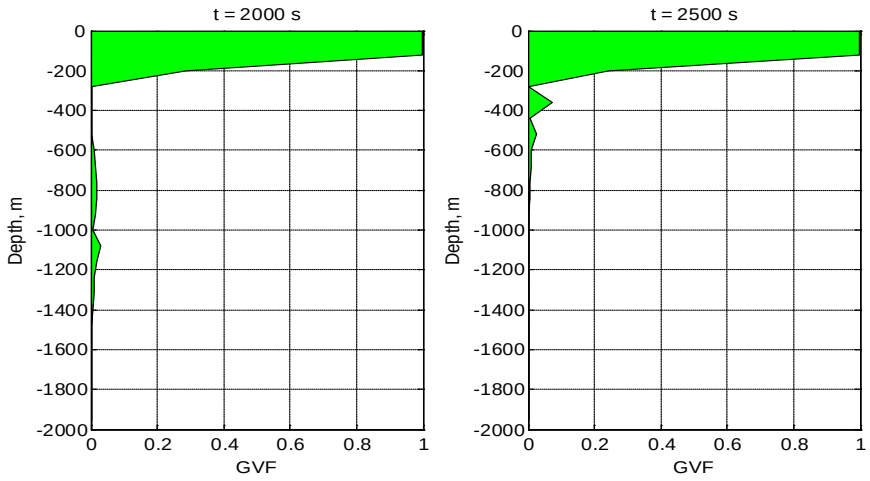

Figure 5.3b—Depth versus gas volume fraction at t = 2000 s and t = 2500 s. Kick volume = 0.5 m^3, number of cells = 25.

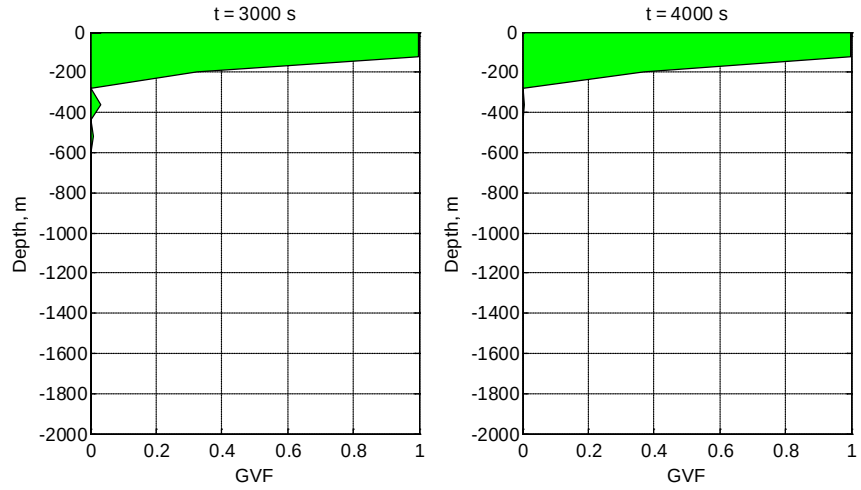

Figure 5.3c—Depth versus gas volume fraction at t = 3000 s and t = 4000 s. Kick volume = 0.5 m^3, number of cells = 25.

In **Fig. 5.3b** (Left), the kick volume appears to shrink, even though the mass is the same. This is caused by the area change, as the kick enters the riser with a much larger cross-sectional area. At 4000 s, a stable air/drilling fluid interface

is restored as shown in **Fig.5.3c** (Right). This time, the gas kick has been circulated out of the system.

Numerical Dissipation. Numerical diffusion affects first order schemes because of the discretization error. The AUSMV scheme—a first order scheme—is also subject to this effect. A simple example will be used to show the effect of numerical discretization on the BHP.
Fig. 5.4 shows plots of BHP versus time for three different cell sizes.

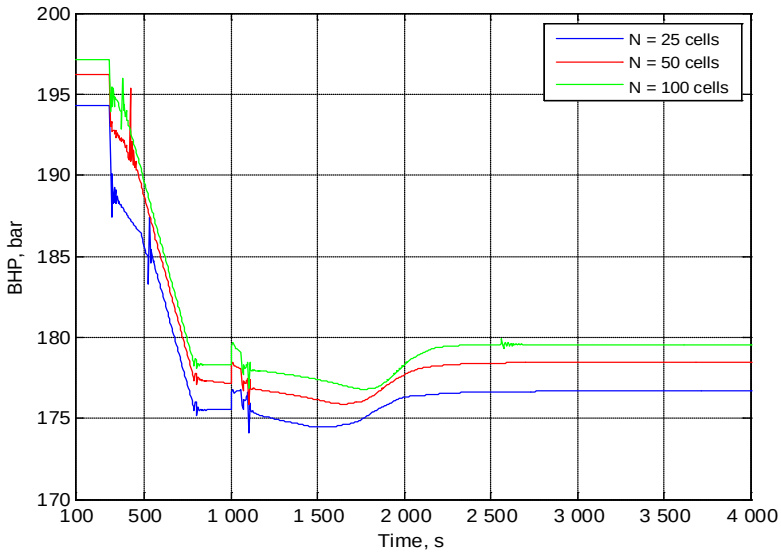

Fig. 5.4—Annular bottomhole pressure versus time. The results show the effect of discretization error on the BHP.

The difference in the results shows that accuracy in the prediction of BHP improves when a higher number of grid cells is used in the simulation. Increasing the cells from 25 to 100, results in a pressure difference of 2 bar at 4000 s. In addition, as the grid is refined, improvement in accuracy decreases for each refinement. This reflects the convergence of the results. Therefore, a large increase in the BHP may not be expected, if the number of cells is set to 400. A cell size smaller than 20 m, or 200 cells, is sufficient for this case.

However, increasing the number of cells to 200 will cause the simulation to go very slow. The convergence will also take much longer time than necessary. Alternatively, the AUSMV scheme can be extended to a higher order scheme with slope limiter techniques (Fjelde et al. 2003; Lorentzen and Fjelde 2005). In this case, a less computational effort will be required, and convergence towards a solution will be faster with few cells.

5.4 Underbalanced Drilling

Case Description. The dynamics of a UBD system will be investigated with the AUSMV scheme. The aim is to demonstrate the scheme can handle highly dynamic multiphase flow systems. The UBD case focuses on the dynamics of hydrostatic-dominated flow versus friction-dominated flow and different connection procedures.

The vertical well considered is 2000 m deep. The inner diameter of the annulus is 8.5" (0.216 m), and the outer diameter of the drill pipe is 5.5" (0.140 m). In this example, the well is discretized into 50 cells.

The drilling fluid is composed of water and a gas with the same properties as the reservoir gas described in Section 5.3. The gas-slip parameters, $C_0 = 1.1$ and $V_d = 0.5$ m/s.

The pore pressure is 160 bar, and the reservoir fluid is a gas with the same properties as the injected gas. The gas is being produced from a fractured zone with a productivity index of 900 m^3/day/ bar.

The annulus is initially filled with water, and the gas is injected into the well at the rate of 120 m^3/s. The liquid-injection rate is 1320 L/min.

Fig. 5.5 shows the annular BHP development with time.

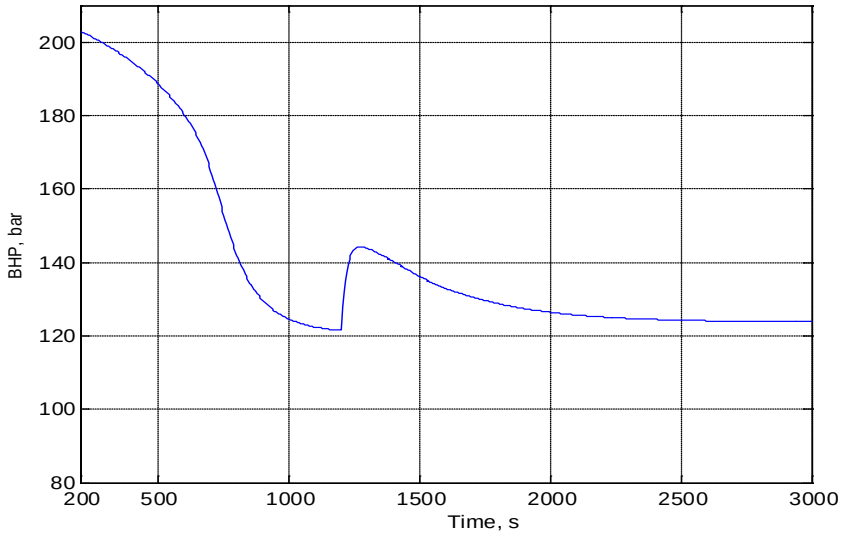

Figure 5.5—The behavior of the annular bottomhole pressure at different simulation time intervals. Choke pressure = 3 bar.

After unloading, the BHP decreases but stabilizes at 122 bar after 1000 s. Before this point, hydrostatic effects dominate the flow conditions. The highly productive fractured zone is drilled at 1200 s. The reservoir gas flows into the well and the annular gas volume increases correspondingly. Then the BHP suddenly increases due to the increase in the annular friction. The flow will approach an optimal point (Saponja 1998), where friction will begin to dominate the pressure conditions.

The BHP gradually decreases as the reservoir gas migrates upward, and the system eventually reaches new steady-state conditions. Thus, the region beyond the point (1200 s, 122 bar) is more friction dominated. This flow condition is more beneficial in controlling the gas influx.

Fig. 5.6 shows that the frictional and hydrostatic components of the BHP approach the optimal point as the system stabilizes.

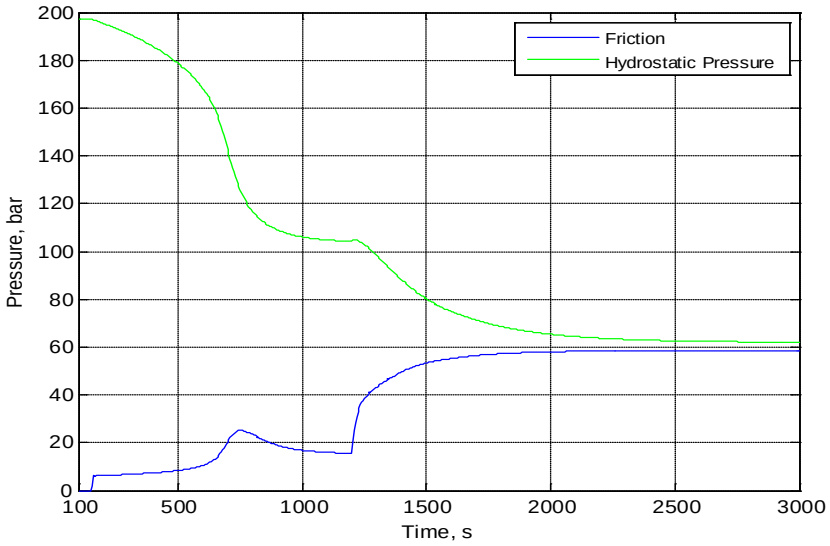

Figure 5.6—Frictional and hydrostatic components of the annular bottomhole pressure.

The BHP (**Fig. 5.5**) is the sum of the frictional and hydrostatic components presented in **Fig. 5.6**. The visual representation of the pressure components in the transient simulations is invaluable because it shows when the pressure condition is hydrostatic or friction dominated.

Effect of Connections. The previous investigation is done without pipe connection. In this section, different connection procedures will be studied, to understand how the BHP will behave in each case.
The pipe connection is performed between 1700 s and 2000 s. Each connection scenario indicates the state of choke opening. For the open connection, the surface backpressure is 3 bar. For the variable connection, the applied choke pressure is gradually increased to 60 bar.
Fig. 5.7 presents the results of the simulations.

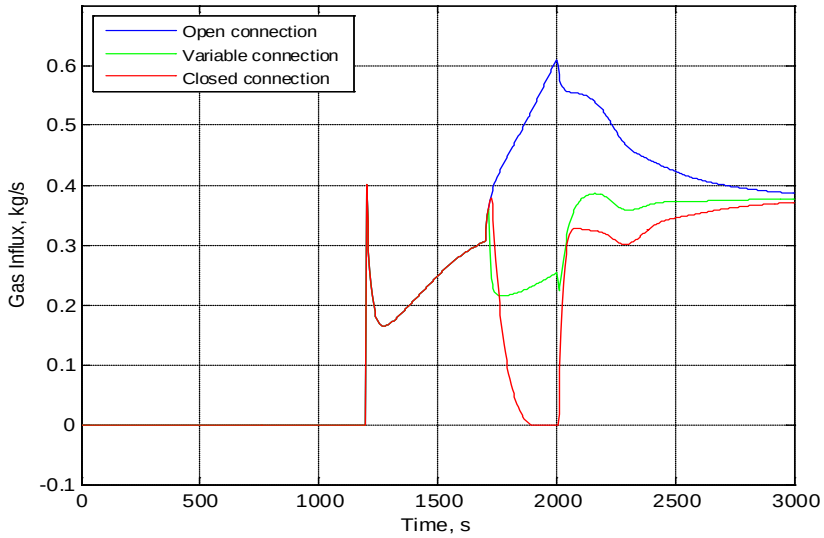

Figure 7.9—Gas influx versus time, for different connection procedures.

From **Fig. 5.7**, it can be observed that the gas influx volume is smallest for the closed connection and largest for the open connection. The variable choke pressure connection has the least fluctuations in the mass influx and is the most advantageous in this example case. This connection procedure also gives the least fluctuation in the BHP as presented in Paper V (**Fig. 14**).
Again, the AUSMV scheme has shown that it is capable of handling the well dynamics associated with pipe connection.

5.5 Inference

Based on the simulation results, the AUSMV scheme has demonstrated that it can handle highly dynamic flow situations associated with DGD and UBD. For the DGD system, the scheme gives insights into the annular BHP behavior and the dynamics of well control.
For the UBD system, the AUSMV scheme is used to study unloading scenario. The scheme is able to predict when steady-state conditions can be achieved. It also shows that it can handle different connection procedures.

The transient model can also be used to investigate the effect of reservoir inflow on the annular BHP. This is important for situations where there are possibilities to encounter highly productive fractured zones.

In addition, the scheme can be used for training and educational purposes. However, it is necessary to consider field data in future works, to prove the practical relevance of the theoretical model. Then, the model predictions can be compared with simulation and experimental results from previous studies.

6 Overview of the Research Papers

Paper I Uncertainty-Based Approach for Predicting the Operating Window in UBO Well Design

The first paper proposes a novel stochastic approach for predicting UBD operational window. Because underbalanced operations involve a highly dynamic flow situation, one inconsistency or the other affects the annular BHP prediction. This can be attributed to modeling uncertainties, which result from the modeling process and input parameters.

This work only considers uncertainties in the flow-dependent parameters such as gas-slip parameters and a factor related to frictional pressure loss gradient. A simple steady-state two-phase model is used to study the UBD system. Probability distributions are assigned to the uncertain inputs, and the uncertainty propagation is by means of Monte Carlo simulation.

Compared with the deterministic method, the simulation results show that the stochastic approach predicts a more realistic operational window. The stochastic model also demonstrates that it has the capability to predict when the BHP is outside the UBD operational limits with a certain probability.

A sensitivity analysis is used to rank the uncertain inputs according to their relative importance. This is based on their individual contributions to the cumulative uncertainty in the BHP. The gas-slip parameters are the most dominant uncertain inputs in this case.

In a way, the stochastic approach can help to reduce uncertainty in the BHP prediction. As a result, well planners can make better decision as they select critical operating parameters during underbalanced drilling.

Paper II Improved Underbalanced Operations with Uncertainty Analysis

This paper is a sequel to **Paper I**. The previous work is conducted without inclusion of reservoir uncertainties. From field experience, there are uncertainties associated with pore pressure prognosis and reservoir inflow performance. There is also uncertainty related to choke operability.

Paper II investigates the cumulative effect of the flow modeling uncertainties—including the uncertainties related to the flow-dependent

parameters—on the BHP prediction. The paper also discusses the uncertainty associated with two-phase flow patterns. However, slug flow is considered as the most dominant flow pattern in this example.

Paper III Uncertainty Evaluation of Wellbore Stability Model Predictions

The paper investigates typical fracture and collapse models with respect to uncertainties in the input parameters. The inputs considered uncertain are in-situ stresses, pore pressure, cohesive rock strength and angle of internal friction. Inaccuracy of the input data may be attributed to noise in measurements and measurement errors. There is a human error as well.

In the stochastic analyses, non-penetrating Kirsch solution for wellbore fracturing and Mohr-Coulomb Shear Failure Criterion for collapse are defined as the base models. The underlying principle is to assign probability distributions to the uncertain input parameters. Then the input uncertainties are propagated by means of Monte Carlo simulation. Traditionally, the deterministic stability models predict single-point estimates of critical fracturing and collapse pressures. In the uncertainty approach, exact solutions become probability distributions.

The sensitivity analyses indicate that the minimum horizontal stress is the most significant random input that influences the critical fracture pressure prediction. For the collapse pressure prediction, the rock cohesive strength is the most dominant input parameter.

A better confidence level can be established because the risks associated with the geopressure prognoses are fully assessed. This may lead to an improved mud window prediction and casing design. Therefore, the approach can improve well planning and help to reduce drilling problems such as lost circulation and stuck pipe.

Paper IV The Academic AUSMV Scheme — A Simple but Robust Model for Predicting Highly Dynamic Well Flow Phenomena

This paper, which is an extended abstract, serves as an introductory paper to **Paper V**. The intent is to present a simple transient flow model that can simulate challenging flow scenarios. The model is based on the drift-flux formulation, and the numerical scheme is of explicit type. The AUSMV scheme has been developed for academic purposes. The modeling algorithm is structured such that students can realize what is behind the modeling process. This scheme has been used in writing many master theses.
Two cases—inspired by UBD transient phenomena—are presented, to show the dynamic capability of the AUSMV scheme.

Paper V A Simple Transient Flow Model for MPD and UBD Applications

This paper presents a simple and robust transient model that can handle highly dynamic flow systems. The model, AUSMV scheme, is developed for academic and training purposes. Students can use the model to investigate different flow scenarios and pressure control challenges encountered in general well control, managed pressure drilling and underbalanced drilling.

The capability of this model to handle highly changing flow scenarios is demonstrated with the examples taken from managed pressure drilling and underbalanced operations.
In the DGD example case, the AUSMV scheme demonstrates that it can simulate a dynamic well control scenario. It is also used in gaining insight into the effects of flow area change and numerical discretization on the annular BHP development.
For the UBD case, the intent is to show the difference between hydrostatic-dominated and friction-dominated flow conditions. The simulation results show how the pressure components can be visualized. In addition, the scheme proves that it can be used to study the dynamic effect related to different connection procedures.

Paper V was revised and submitted to *SPE Drilling & Completion*, with a revised title:
On the AUSMV Scheme: A Simple Transient Flow Model for MPD and UBD Applications.

Paper VI Mud Losses in Fractured Carbonate Formations

This paper was first submitted as a report, in fulfillment of requirements for passing the course—Dual Porosity Reservoirs—organized by Petroleum Research School of Norway (NFiP). It was also presented at the 4th NFiP annual oneday PhD seminar held in Stavanger.

The paper discusses some interconnected factors that are responsible for excessive mud losses in naturally fractured carbonate formations. Such determining factors include wetting condition of a reservoir, drilling fluid selection, and drilling technique. Beside mud losses through fracture pathways, mud can also be lost to the adjacent matrix through spontaneous imbibition process.

Therefore, drilling engineers should consider the wetting conditions and other petrophysical properties of naturally fractured carbonates while deciding on drilling fluid. This can help to reduce mud losses due to spontaneous imbibition.

Proper fracture identification is also very important, to understand how factures are distributed in a formation. Where it is not viable to drill with a conventional method, managed pressure drilling or underbalanced operations can be the only option to harness the target.

7 Conclusion and Further Work

7.1 Conclusion

This work presents a novel stochastic approach for drilling and well planning. Some vital operational concerns have motivated the proposition of the methodology.
Mathematical models are but perfect tools for investigating subsurface phenomena, processes and so forth. This also applies to hydraulic flow models and wellbore stability models. Generally, modeling uncertainties may result from uncertainties in input parameters. The input uncertainties may be due to noise in measurements and measurement errors. There is a human error as well. In some situations, the input data are scarce and inadequate. In addition, there is uncertainty resulting from modeling processes, because models only approximate physical phenomena.

Drilling engineers often use deterministic and scenario methods, to determine critical operational parameters. Because the methods are based on the deterministic formulation, they only give single-point estimates of the parameters. Put differently, they lack the capacity to propagate uncertainty. As a result, vital information about the output variabilities is lost, and the associated risks are not fully explored.

The proposed stochastic approach provides an alternative drilling and well planning approach. This approach is simple and easy to implement. Here, exact solutions become probability distributions, and the uncertainty propagation is by means of Monte Carlo simulation. The uncertainty approach has been applied in the well planning of UBO and wellbore stability analyses.
In wellbore stability analyses, single-point estimates of the critical fracturing and collapse pressure may give too optimistic a mud window. The stochastic approach shows that it can be a useful tool for assessing risks and uncertainties associated with the geopressure predictions.
The probabilistic modeling of the underbalanced operations gives a different recommendation—on the operational window—from the deterministic method. The stochastic model is able to predict when the annular BHP is outside the UBD operational limits with a certain probability.

Judging from the foregoing discussion, the stochastic modeling may be a future and cost-efficient drilling solution for exploiting depleted reservoirs, fractured carbonate formations and deepwater targets. In essence, the industry will always use deterministic and scenario methods. Yet their predictions should be supplemented with the results from stochastic simulations.

This work also presented a one-dimensional, two-phase transient model termed the AUSMV scheme. The explicit scheme can be used to study the dynamics of various transient scenarios, for different drilling technologies. The flow model has some potential that can be relevant to educational purposes. It can be used to study the dynamics of different drilling systems.
The capability of the scheme to simulate highly dynamic phenomena is presented for dual-gradient drilling and underbalanced operations.
In the DGD example case, the AUSMV scheme demonstrates that it can simulate a dynamic well control scenario. It is also used in gaining insight into the effects of flow area change and numerical discretization on the annular BHP development.
For the UBD case, the intent is to show the difference between hydrostatic-dominated and friction-dominated flow conditions. The simulation results show how the pressure components can be visualized. In addition, the scheme proves that it can be used to study the dynamic effect related to different connection procedures.

7.2 Further Work

The flow models used in this work are formulated under isothermal conditions. This assumption is at variance with real downhole conditions, because wellbore temperature affects multiphase variables such as viscosity and density. Future works should consider thermal effects. As a result, more advanced closure laws will be used to improve the accuracy of the two-phase flow models.

As flow-dependent variables, the values of the slip parameters, C_0 and V_d, depend on the prevailing two-phase flow pattern. It is then pertinent to implement the mechanistic models, described in Lage and Time 2000, in the steady-state flow model. With this, the most uncertain flow pattern can be determined, and more accurate values of the slip parameters can be used.

Generally, the input distributions should be chosen such that they reflect the physics of the problem. No formal test is performed in this work, to determine the goodness of fit of the input distributions and convergence of the model results. The focus here is to present a simple stochastic approach for drilling and well planning.
Investigating the goodness of fit of the input distributions should be discussed in a future study. This can be performed with Cramér-von Mises Criterion (Anderson 1962) or any other formal tests. Therefore, more literature and experimental data should be considered, to ascertain what could be the most appropriate distributions for the uncertain input parameters.

Another area that requires further research is calibration of AUSMV scheme with real data. The model must be extended to a second order scheme, to reduce the simulation time and improve the prediction accuracy. In addition, the effect of numerical discretization should be discussed in detail. Then, it will be pertinent to compare the model's predictions with simulation and experimental results from previous studies.

Finally, one can integrate the steady-state flow model with the geopressure models and investigate the integrated system with the probabilistic approach.

References

Aadnøy, B.S. 1988. Inversion Technique to Determine the In-Situ Stress Field from Fracturing Data. Paper SPE 18023, presented at the 63rd SPE Annual Technical Conference and Exhibition, Houston, Texas, USA, 2–5 October. http://dx.doi.org/10.2118/18023-MS.

Aadnøy, B.S. 2010. *Modern Well Design*, second edition. Leiden, The Netherlands: CRC Press/Balkema.

Aadnøy, B.S. 2011. Quality Assurance of Wellbore Stability Analyses. Paper SPE 140205, presented at the SPE/IADC Drilling Conference and Exhibition, Amsterdam, The Netherlands, 1–3 March. http://dx.doi.org/10.2118/140205-MS.

Aadnøy, B.S. and Chenevert, M.E. 1987. Stability of Highly Inclined Boreholes. *SPE Drill Eng* **4** (2): 368–374. http://dx.doi.org/10.2118/16052-PA.

Aadnøy, B.S., Cooper, I., Miska, S.Z., Mitchell, R.F, and Payne, M.L. 2009. *Advanced Drilling and Well Technology*. Richardson, Texas, USA: Society of Petroleum Engineers.

Aadnøy, B.S. and Hansen, A.K. 2005. Bounds on In-Situ Stress Magnitudes Improve Wellbore Stability Analyses. *SPE Journal* **10** (2): 115–120. http://dx.doi.org/10.2118/87223-PA.

Aadnøy, B.S. and Looyeh, R. 2010. *Petroleum Rock Mechanics: Drilling Operations and Well Design.* Oxford, UK: Gulf Professional Publishing.

Adams, A.J., Gibson, C., and Smith, R. 2010. Probabilistic Well-Time Estimation Revisited. *SPE Drill & Compl* **25** (4): 472–499. http://dx.doi.org/10.2118/119287-PA.

Adams, A.J, Parfitt, S.H.L., Reeves, T.B., Thorogood, J.L. 1993. Casing System Risk Analysis Using Structural Reliability. Paper SPE 25693, presented

at the 1993 SPE/IADC Drilling Conference, Amsterdam, Netherlands, 23–25 February. http://dx.doi.org/10.2118/25693-MS.

Addis, M.A., Hanssen, T.H, Yassir, N., Willoughby, D.R, and Enever, J. 1998. A Comparison of Leak-off Test and Extended Leak-off Test Data for Stress Estimation. Paper SPE 47235, presented at the SPE/ISRM Eurock 98, Trondheim, Norway, 8–10 July. http://dx.doi.org/10.2118/47235-MS.

Anderson, E.M., 2012. The Dynamics of Faulting. *The Geological Society, London, Special Pubs.* **367** (1): 231–246. http://dx.doi.org/10.1144/SP367.16.

Anderson, T.W. 1962. On the Distribution of the Two-Sample Cramér-von Mises Criterion. *Ann. Math. Statist.* **33** (3): 1148–1159. http://dx.doi.org/10.1214/aoms/1177704477.

Arild, Ø., Fjelde, K.K., Merlo, A., and Løberg, T. 2008. BlowFlow — A New Tool within Blowout Risk Management. Paper SPE 114568, presented at IADC/SPE Asia Pacific Drilling Technology Conference and Exhibition, Jakarta, Indonesia, 25–27 August. http://dx.doi.org/10.2118/114568-MS.

Arild, Ø., Ford, E.P., Løberg, T., and Baringbing, J.W.T. 2009. KickRisk — A Well Specific Approach to the Quantification of Well Control Risks. Paper SPE 124024, presented at the SPE Asia Pacific Oil and Gas Conference and Exhibition, Jakarta, Indonesia, 4–6 August. http://dx.doi.org/10.2118/124024-MS.

Bennion, D.B. and Thomas, F.B. 1994. Underbalanced Drilling of Horizontal Wells: Does It Really Eliminate Formation Damage? Paper SPE 27352, presented at the SPE Intl. Symposium on Formation Damage Control, Lafayette, Louisiana, 7–10 February. http://dx.doi.org/10.2118/27352-MS.

Bennion, D.B., Thomas, F.B., Bietz, R.F., and Bennion, W.D. 1998. Underbalanced Drilling, Praises and Perils. *SPE Drill & Compl* **13**(4): 214–222. http://dx.doi.org/10.2118/52889-PA.

Bradley, W.B. 1979. Failure of Inclined Boreholes. *J. Energy Resources Technology* **101** (4): 232–239. http://dx.doi.org/10.1115/1.3446925.

Bratvold, R.B. and Begg, S.H., 2010. *Making Good Decisions*. Richardson, Texas, USA: Society of Petroleum Engineers.

Breyholtz, Ø. 2011. Managed Pressure Drilling: Improved Pressure Control through Model Predictive Control. PhD thesis, University of Stavanger, Norway.

Brown, J.D, Urvant, V.V., Thorogood, J.L., and Rolland, N.L. 2007. Deployment of a Riserless Mud-Recovery System Offshore Sakhalin Island. Paper SPE 105212, presented at SPE/IADC Drilling Conference, Amsterdam, The Netherlands, 20–22 February. http://dx.doi.org/10.2118/105212-MS.

Caetano, E.F. 1986. Upward Two-Phase Flow through an Annulus. PhD thesis, University of Tulsa, USA.

Cohen, J.H. and Deskins, G. 2006. Use of lightweight Solid additives to Reduce the Weight of Drilling Fluid in the Riser. Paper SPE 99174, presented at the IADC/SPE Drilling Conference, Miami, Florida, USA, 21–23 February. http://dx.doi.org/10.2118/99174-MS.

Cunha, J.C. and Rosa, F.S.N. 1998. Underbalanced Drilling Technique Improves Drilling Performance — a Field Case History. Paper SPE 47802, presented at the IADC/SPE Asia Pacific Drilling Conference, Jakarta, Indonesia, 7–9 September. http://dx.doi.org/10.2118/47802-MS.

De Fontoura, S.A.B., Holzberg, B.B., Teixeira E.C., and Frydman, M. 2002. Probabilistic Analysis of Wellbore Stability during Drilling. Paper SPE 78179, presented at the SPE/ISRM Rock Mechanics Conference, Irving, Texas, 20–23 October. http://dx.doi.org/10.2118/78179-MS.

De Rocquigny, E., Devictor, N., and Tarantola, S. eds. 2008. *Uncertainty in Industrial Practice: A Guide to Quantitative Uncertainty Management*. Chichester, UK: John Wiley & Sons Ltd.

De Rocquigny, E. 2009. Quantifying Uncertainty in an Industrial Approach: An Emerging Consensus in an Old Epistemological Debate. S.A.P.I.E.N.S **2** (1). http://sapiens.revues.org/782.

Dowell, J.D. 2010. Deploying the World's First Commercial Dual-Gradient System. Paper SPE 137319, presented at the SPE Deepwater Drilling and Completions Conference, Galveston, Texas, USA, 5–6 October. http://dx.doi.org/10.2118/137319-MS.

Eggemeyer, J.C., Akins, M.E., Brainard, R.R., et al. 2001. SubSea MudLift Drilling: Design and Implementation of a Dual-Gradient Drilling System. Paper SPE 71359, presented at the 2001 SPE Annual Technical Conference and Exhibition, New Orleans, Louisiana, USA, 30 September–3 October. http://dx.doi.org/10.2118/71359-MS.

Evje, S. and Fjelde, K.K. 2002. Hybrid Flux-Splitting Schemes for a Two-Phase Flow Model. *J. Computational Physics.* **175** (2) 674–701. http://dx.doi.org/10.1006/jcph.2001.6962.

Evje, S. and Fjelde, K.K. 2003. On a Rough AUSM Scheme for a One-Dimensional Two-Phase Model. *Computers & Fluids J.* **32** (10): 1497–1530. http://dx.doi.org/10.1016/S0045-7930(02)00113-5.

Falk, K., Fossli, B., Lagerberg, C., Handal, A., and Sangesland, S. 2011. Well Control When Drilling with a Partly Evacuated Marine Drilling Riser. Paper SPE 143095, presented at the IADC/SPE Managed Pressure Drilling and Underbalanced Operations Conference and Exhibition, Denver, Colorado, USA, 5–6 April. http://dx.doi.org/10.2118/143095-MS.

Fjelde, K.K., Rommetveit, R., Merlo, A, and Lage, A.C.V.M. 2003. Improvements in Dynamic Modeling of Underbalanced Drilling. Paper SPE 81636, presented at the IADC/SPE Underbalanced Technology Conference and Exhibition, Houston, Texas, USA, 25–26 March. http://dx.doi.org/10.2118/81636-MS.

Forrest, N. and Bailey, T. 2001. Subsea Equipment for Deep Water Drilling Using Dual Gradient Mud System. Paper SPE 67707, presented at the SPE/IADC Drilling Conference, Amsterdam, The Netherlands, 27 February–1 March. http://dx.doi.org/10.2118/67707-MS.

Fossli, B. and Sangesland, S. 2006. Controlled Mud-Cap Drilling for Subsea Applications: Well Control Challenges in Deep Waters. *SPE Drill & Compl* **21** (2): 133–140. http://dx.doi.org/10.2118/91633-PA.

Gerald, C.F and Wheatley, P.O. 2004. *Applied Numerical Analysis*, seventh edition. Boston, Massachusetts: Addison-Wesley Publishing Company.

Gough, G., Talbot, S., and Moos H. 2011. Offshore Underbalanced Drilling with a Closed-Loop Circulating System. Paper SPE 143096, presented at the IADC/SPE Managed Pressure Drilling and Underbalanced Operations Conference and Exhibition, Denver, Colorado, USA, 5–6 April. http://dx.doi.org/10.2118/143096-MS.

Handal, A. 2011. Gas Influx Handling for Dual Gradient Drilling. PhD thesis, Norwegian University of Science and Technology, Trondheim, Norway.

Harten, A., Lax, P.D, van Leer, B. 1983. On Upstream Differencing and Godunov Schemes for Hyperbolic Conservation Laws. *SIAM Review* **25** (1): 35–61. http://dx.doi.org/10.1137/1025002.

Kosh, G.S. and Link, R.F. 1980. *Statistical Analysis of Geological data*, volume 1. New York, USA: Dover Publications, Inc.

Lage, A.C.V.M. 2000. Two-Phase Flow Models and Experiments for Low-Head and Underbalanced Drilling. PhD thesis, University of Stavanger, Stavanger, Norway

Lage, A.C.V.M., Fjelde, K.K., and Time, R.W. 2003. Underbalanced Drilling Dynamics: Two-Phase Flow Modeling and Experiments. *SPE Journal* **8** (1): 61–70 http://dx.doi.org/10.2118/62743-MS.

Lage, A.C.V.M. and Time, R.W., 2000. An Experimental and Theoretical Investigation of Upward Two-Phase Flow in Annuli. Paper SPE 64525, presented at the SPE Asia Pacific Oil and Gas Conference and Exhibition, Brisbane, Australia, 16-18 October. http://dx.doi.org/10.2118/64525-MS.

Liang, Q.J. 2002. Application of Quantitative Risk Analysis to Pore Pressure and Fracture Gradient Prediction. Paper SPE 77354, presented at the SPE Annual Technical Conference and Exhibition, San Antonio, Texas, USA, 29 September–2 October. http://dx.doi.org/10.2118/77354-MS.

Liou, M.-S. 1996. A Sequel to AUSM: AUSM+. *J. Comput. Phys.* **129** (2): 364–382. http://dx.doi.org/10.1006/jcph.1996.0256.

Liou, M.-S. and Steffen, C.J. 1993. A New Flux Splitting Scheme. *J. Comput Phys.* **107** (1): 23–34. http://dx.doi.org/10.1006/jcph.1993.1122.

Livescu, S., Durlofsky, L.J., Aziz, K., and Ginestra, J.C. 2009. A Fully-Coupled Thermal Multiphase Wellbore Flow Model for Use in Reservoir Simulation. *J. Pet. Sci. Eng.* **71** (2–3): 138–146. http://dx.doi.org/10.1016/j.petrol.2009.11.022.

Lopes, C.A. and Bourgoyne, A.T. 1997. The Dual Density Riser Solution. Paper SPE 37628, presented at the 1997 SPE/IADC Drilling Conference, Amsterdam, The Netherlands, 4–6 March. http://dx.doi.org/10.2118/37628-MS.

Lorentzen, R.J. and Fjelde, K.K. 2005. Use of Slopelimiter Techniques in Traditional Numerical methods for Multi-phase Flow in Pipelines and Wells. *Int. J. Num. Meth. Fluids* **48** (7): 723–745. http://dx.doi.org/10.1002/fld.952.

Løberg, T., Arild, Ø., Merlo, A., and D'Alesio, P. 2008. The How's and Whys of Probabilistic Well Cost Estimation. Paper SPE 114696, presented at the IADC/SPE Asia Pacific Drilling Technology Conference and Exhibition, Jakarta, Indonesia, 25–27 August. http://dx.doi.org/10.2118/114696-MS.

Masella, J-M., Faille, I., and Gallouet, T. 1999. On an Approximate Godunov Scheme. International *J. Comput. Fluid Dynamics* **12** (2): 133–149. http://dx.doi.org/10.1080/10618569908940819.

Moors, k. 2011. *The Vega Factor*. Hoboken, New Jersey: John Wiley & Sons.

Morita, N. 1995. Uncertainty Analysis of Borehole Stability Problems. Paper SPE 30502, presented at the SPE Annual Technical Conference & Exhibition, Dallas, Texas, USA, 22–25 October. http://dx.doi.org/10.2118/30502-MS.

Mostafavi, V., Aadnøy, B.S., and Hareland, G. 2011. Model-Based Uncertainty Assessment of Wellbore Stability Analyses and Downhole Pressure Estimations. Paper ARMA 11-127, presented at the 45th US Rock Mechanics / Geomechanics Symposium, San Francisco, CA, 26–29 June.

Murtha, J.A. 1997. Monte Carlo Simulation: Its Status and Future. *J Pet. Tech.* **49** (4) 361–373. http://dx.doi.org/10.2118/37932-JPT.

Mykytiw, C., Suryanarayana, P.V., and Brand, P.R. 2004. Underbalanced Drilling Applications Designs—the Tricks of the Trade. Paper SPE 91598, presented at the 2004 SPE/IADC Underbalanced Technology Conference and Exhibition, Houston, Texas, USA, 11–12 October. http://dx.doi.org/10.2118/91598-MS.

Nas, S. 2010. Offshore Managed-Pressure Drilling Boosts Efficiency in Asia Pacific. *Exploration & Production*. http://www.epmag.com/Production-Drilling/Offshore-managed-pressure-drilling-boosts-efficiency-Asia-Pacific_52437 (accessed 23 June 2014).

Nersesian, R. 2013. *Energy Risk Modeling*. New York, USA: Palisade Corporation.

Nilsen, T., Sandøy, M., Rommetveit, R., and Guarneri, A. 2001. Risk-Based Well Control Planning: The Integration of Random and Known Quantities in a Computerized Risk management Tool. Paper SPE 68447, presented at the SPE/ICoTA Coiled Tubing Roundtable, Houston, Texas, 7–8 March. http://dx.doi.org/10.2118/68447-MS.

Osayande, N., Mammadov, E., Sephton, S., and Boucher, V. 2014. The Successful Application of Automated Managed Pressure Drilling (MPD) to Protect Cap Rock Integrity by Narrow margin Drilling in SAGD Wells. Paper

SPE 170152, presented at the SPE Heavy Oil Conference-Canada, Alberta, Canada, 10–12 June. http://dx.doi.org/10.2118/170152-MS.

Osher, S. 1984. Riemann Solvers, the Entropy Conditions, and Difference Approximations. *SIAM J. Numerical Analysis* **21** (2): 217–235. http://www.jstor.org/stable/2157297.

Ottesen, S, Zheng, R.H., and McCann, R.C. 1999. Borehole Stability Assessment Using Quantitative Risk Analysis. Paper SPE 52864, presented at the SPE/IADC Drilling Conference, Amsterdam, Netherlands, 9–11 March. http://dx.doi.org/10.2118/52864-MS.

Petoro. 2014. Press Conference, First Quarter 2014. http://www.petoro.no/Hva%20vi%20sier/presentasjoner/Pressekonferanse-Q1-2014-4.pdf (accessed 21 May 2014).

Rahman, S.S. and Chilingarian, G.V. 1995. *Casing Design—Theory and Practice*. Amsterdam, The Netherlands: Elsevier Science.

Rajabi, M.M., Toftevåg, K., Stave, R.S, and Ziegler, R. 2012. First Application of EC-Drill in Ultra-Deepwater—Proven Subsea Managed Pressure Drilling Method. Paper SPE 151100, presented at the SPE Deepwater Drilling and Completions Conference, Galveston, Texas, USA, 20–21 June. http://dx.doi.org/10.2118/151100-MS.

Ramalho, J. and Davidson, I.A. 2006. Well-Control Aspects of Underbalanced Drilling Operations. Paper SPE 106367, presented at the IADC/SPE Asia Pacific Drilling Technology Conference and Exhibition, Bangkok, Thailand, 13–13 November. http://dx.doi.org/10.2118/106367-MS.

Rehm, B., Schubert, J., Haghshenas, A., Paknejad, A.S., and Hughes, J. eds. *Managed Pressure Drilling*. Houston, Texas: Gulf Publishing Company.

Roe, P.L. 1980. The Use of the Riemann Problem in Finite Difference Schemes. *Lecture Notes in Physics* vol. **141**: 354–359. http://link.springer.com/chapter/10.1007/3-540-10694-4_54.

Roe, P.L. 1981 Approximate Riemann Solvers, Parameter Vectors, and Difference Schemes. *J. Comput. Phys.* **43** (2): 357–372. http://dx.doi.org/10.1016/0021-9991(81)90128-5.

Romate J.E. 1998. An Approximate Solver for a Two-Phase Flow Model with Numerically Given Slip Relation. *Computers & Fluids* 27(4): 455–477. http://dx.doi.org/10.1016/S0045-7930(97)00067-4.

Rommetveit, R., Fjelde, K.K., Aas, B, et al. 2003. HPHT Well Control; An Integrated Approach. Paper OTC 15322, presented at the 1997 Offshore Technology Conference, Houston, Texas, USA, 5–8 May. http://dx.doi.org/10.4043/15322-MS.

Rommetveit, R., Fjelde, K.K., Frøyen, J., et al. 2004. Use of Dynamic Modeling in Preparations for the Gullfaks C-5A Well. Paper SPE 91243, presented at 2004 SPE/IADC Underbalanced Technology Conference and Exhibition, Houston, Texas, USA, 11-12 October. http://dx.doi.org/10.2118/91243-MS.

Rommetveit, R., Sævareid, O., Lage, A.C.V.M, et al. 1999. Dynamic Underbalanced Drilling Effects are Predicted by Design Model. Paper SPE 56920, presented at the 1999 Offshore Europe Conference, Aberdeen, Scotland, 7–9 September. http://dx.doi.org/10.2118/56920-MS.

Saltelli, A., Chan, K., and Scott, E.M. eds. 2008. *Sensitivity Analysis*. Chichester, UK: John Wiley & Sons, Ltd.

Saponja, J. 1998. Challenges with Jointed-Pipe Underbalanced Operations. *SPE Drill & Compl* **13** (2): 121–128. http://dx.doi.org/10.2118/37066-PA.

Schubert, J.J., Juvkam-Wold, H.C., and Choe, J. 2006. Well-Control Procedures for Dual-Gradient Drilling as Compared to Conventional Riser Drilling. *SPE Drill & Compl* **21** (4): 287–295. http://dx.doi.org/10.2118/99029-PA.

Schumacher, J.P., Dowell, J.D, Ribbeck, L.R, and Eggemeyer, J.C. 2001. SubSea MudLift Drilling: Planning and Preparation for the First SubSea Field

Test of a Full-scale Dual-Gradient Drilling System at Green Canyon 136, Gulf of Mexico. Paper SPE 71358, presented at the 2001 SPE Annual Technical Conference and Exhibition, New Orleans, Louisiana, USA, 30 September–3 October. http://dx.doi.org/10.2118/71358-MS.

Schumacher, J.P., Dowell, J.D., Ribbeck, L.R., and Eggemeyer, J.C. 2002. Planning and Preparing for the First Subsea field Test of a Full-Scale Dual-Gradient Drilling System. *SPE Drill & Compl* **17** (4): 194–199. http://dx.doi.org/10.2118/80615-PA.

Sheng, Y., Reddish, D., and Lu, Z. 2006. Assessment of Uncertainties in Wellbore Stability Analysis. *Modern Trends in Geomechanics, Springer Proceedings in Physics* **106** (6): 541–557. http://dx.doi.org/10.1007/978-3-540-35724-7_31.

Stave, R., Farestveit, R., Høyland, S., Rochmann, P.O., and Rolland, N.L. 2005. Demonstration and Quantification of a Riserless Dual Gradient System. Paper OTC 17665, presented at the 2005 offshore Technology Conference, Houston Texas, USA, 2–5 May. http://dx.doi.org/10.4043/17665-MS.

Udegbunam, J.E., Aadnøy, B.S., and Fjelde, K.K. 2013a. Paper SPE 166788, presented at the SPE/IADC Middle East Drilling Technology Conference and Exhibition, Dubai, 7–9 October. http://dx.doi.org/10.2118/166788-MS.

Udegbunam, J.E, Arild, Ø., Fjelde, K.K., Ford, E., and Lohne, H.P. 2013b. Uncertainty-Based Approach for Predicting the Operating Window in UBO Design. *SPE Drill & Compl* **28** (4): 326–337. http://dx.doi.org/10.2118/164916-PA.

Udegbunam, J.E., Fjelde, K.K., Steinar, E., and Nygaard, G. 2014. A simple Transient Flow Model for MPD and UBD Applications. Paper SPE 168960, presented at the SPE/IADC Managed Pressure Drilling and Underbalanced Operations Conference and Exhibition, Madrid, Spain, 8–9 April. http://dx.doi.org/10.2118/168960-MS.

Walpole, R.E., Myers, R.H., Myers, S.L, and Ye, K. 2012. *Probability & Statistics for Engineers and Scientist*, ninth edition. Boston, USA: Pearson Education, Inc.

Williamson, H.S., Sawaryn, S.J., and Morrison, J.W. 2006. Monte Carlo Techniques Applied to Well Forecasting: Some Pitfalls. *SPE Drill & Compl* **21** (3): 216–277. http://dx.doi.org/10.2118/89984-PA.

Zuber, N and Findlay, J.A. 1965. Average Volumetric Concentration in Two-Phase Flow Systems. *J. Heat Transfer* **87** (4): 453–468. http://dx.doi.org/10.1115/1.3689137.

Papers not included due to copyright.
See page VII for references.